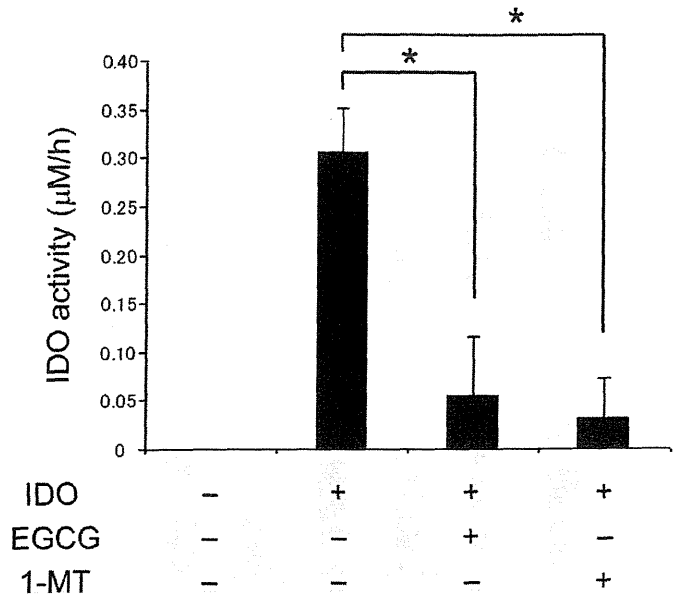

Fig. 6. Effects of 1-methyltryptophan (1-MT) and (−)-epigallocatechin gallate (EGCG) on indoleamine 2,3-dioxygenase (IDO) activity in cell-free assays. Functional activity of recombinant human IDO enzyme in response to 1-MT and EGCG was determined by measuring the concentrations of enzymatic products (L-kynurenine) using HPLC. Enzymatic activity is expressed as the product content per hour (μM/h). Data are the mean ± SD. *P < 0.001.

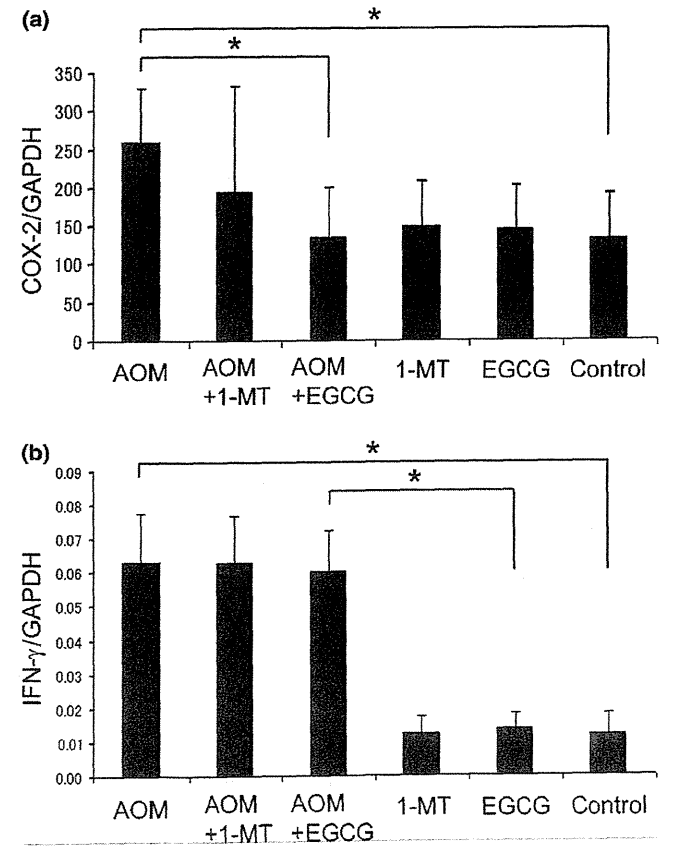

Fig. 7. Effects of 1-methyltryptophan (1-MT) and (−)-epigallocatechin gallate (EGCG) on the expression of (a) cyclooxygenase (COX)-2 and (b) interferon (IFN)-γ in stromal cells, as determined by quantitative RT-PCR. Expression is normalized against that of GAPDH. AOM, azoxymethane. Data are the mean ± SD (n = 6). *P < 0.05.

immune cells in the stroma, are related to IDO expression.[38] In addition, several other immune regulatory factors have been implicated as inducers of IDO, including COX-2, which is regarded as one of the most critical inflammatory mediators in the regulation of IDO expression.[42] In the present study, the AOM-induced upregulation of COX-2 in the colonic stroma of rats was significantly inhibited by the administration of EGCG (Fig. 7a). These findings, together with those of Basu *et al.*,[43] who reported a suppressive role of a COX-2 inhibitor against IDO expression in the tumor microenvironment, suggest that EGCG inhibits the expression of IDO, possibly by preventing the induction of COX-2, although further investigations are required to clarify the effects of EGCG. Thus, combination treatment using an IDO inhibitor plus a COX-2 inhibitor may be an effective regimen for the chemoprevention of colorectal cancer because this combination will synergistically inhibit the expression and activity of IDO.

Interferon-γ is also thought to be a major stimulator of IDO,[40,41] and EGCG has been reported to suppress IDO expression by inhibiting STAT-1 activation in response to IFN-γ *in vitro*.[23,24] However, in the present study the expression of IFN-γ in the colonic stroma was not affected by EGCG in the drinking water (Fig. 7b). Other novel mechanisms by which EGCG modulates the expression of IDO may exist; therefore, further studies are needed to clarify the effects of EGCG on the immunoregulatory pathways related to IDO expression.

Aberrant crypt foci have attracted attention as putative precancerous lesions of the colon in experimental models.[48] Numerous molecular abnormalities, including increased expression of K-*ras* and *APC* gene mutations, have been demonstrated in human ACF.[49] In addition, BCAC, which accumulate β-catenin protein in the nucleus and cytoplasm, are regarded as putative precursors to colorectal adenomas.[50] Several rodent studies have shown that both these lesions are useful as biomarkers to evaluate the chemopreventive properties of specific agents.[19,36,37,51] Therefore, our findings, namely that both 1-MT and EGCG markedly inhibit the development of ACF and BCAC, appear to be significant when considering the chemoprevention of colorectal cancer. In particular, a significant reduction of large ACF by 1-MT and EGCG should be emphasized, because large ACF are known to have a strong correlation with the incidence of colonic adenocarcinoma.[20,21]

Finally, it should be mentioned that one limitation of the present study was that the L-kynurenine/L-tryptophan ratio may not directly reflect IDO activity because kynurenine can be metabolized further and TDO can also produce kynurenine from tryptophan.[12] However, in the present study we presumed that TDO exerted little effect on L-kynurenine levels because the expression of TDO was not affected by AOM treatment (Fig. 4c,d). Systemic IDO activity is currently estimated by the serum L-kynurenine/L-tryptophan ratio,[33] as in the present study, because IDO is an intracellular enzyme and circulating IDO concentrations are barely detectable.[3] In fact, a method for analyzing serum IDO protein itself has not been established in experimental animals and there is only one report, published in 2012, of its detection in humans.[52] This limitation needs to be addressed in future studies.

In conclusion, the escape of precancerous cells from the immune system caused by immune tolerance is involved in certain types of carcinogenesis and, therefore, may be an effective target for the implementation of chemoprevention. The results of the present study support the notion that IDO upregulation, which induces immune tolerance, contributes to the early phase of colon carcinogenesis. Furthermore, the present study is the first to provide evidence that the anti-carcinogenic properties of 1-MT and EGCG may be related to inhibition of

doi: 10.1111/j.1349-7006.2012.02237.x

IDO activity, suggesting that targeting IDO and correcting IDO-mediated immune tolerance with EGCG or an IDO inhibitor could be a promising strategy for the prevention of colorectal cancer development in the future. Further experiments using IDO-knockout mice would strengthen the connection between IDO activity and the development of colorectal cancer, and may prove useful in the exploration of IDO inhibitors as chemopreventive agents for colorectal cancer.

Acknowledgment

The authors thank Mitsui Norin (Tokyo, Japan) for providing the EGCG.

Disclosure Statement

The authors have no conflicts of interest to declare.

References

1 Zitvogel L, Tesniere A, Kroemer G. Cancer despite immunosurveillance: immunoselection and immunosubversion. *Nat Rev Immunol* 2006; 6: 715–27.
2 Uyttenhove C, Pilotte L, Theate I *et al.* Evidence for a tumoral immune resistance mechanism based on tryptophan degradation by indoleamine 2,3-dioxygenase. *Nat Med* 2003; 9: 1269–74.
3 Mellor AL, Munn DH. IDO expression by dendritic cells: tolerance and tryptophan catabolism. *Nat Rev Immunol* 2004; 4: 762–74.
4 Frumento G, Rotondo R, Tonetti M, Damonte G, Benatti U, Ferrara GB. Tryptophan-derived catabolites are responsible for inhibition of T and natural killer cell proliferation induced by indoleamine 2,3-dioxygenase. *J Exp Med* 2002; 196: 459–68.
5 Okamoto A, Nikaido T, Ochiai K *et al.* Indoleamine 2,3-dioxygenase serves as a marker of poor prognosis in gene expression profiles of serous ovarian cancer cells. *Clin Cancer Res* 2005; 11: 6030–9.
6 Ino K, Yoshida N, Kajiyama H *et al.* Indoleamine 2,3-dioxygenase is a novel prognostic indicator for endometrial cancer. *Br J Cancer* 2006; 95: 1555–61.
7 Brandacher G, Perathoner A, Ladurner R *et al.* Prognostic value of indoleamine 2,3-dioxygenase expression in colorectal cancer: effect on tumor-infiltrating T cells. *Clin Cancer Res* 2006; 12: 1144–51.
8 Ninomiya S, Hara T, Tsurumi H *et al.* Indoleamine 2,3-dioxygenase in tumor tissue indicates prognosis in patients with diffuse large B-cell lymphoma treated with R-CHOP. *Ann Hematol* 2010; 90: 409–16.
9 Yoshikawa T, Hara T, Tsurumi H *et al.* Serum concentration of L-kynurenine predicts the clinical outcome of patients with diffuse large B-cell lymphoma treated with R-CHOP. *Eur J Haematol* 2010; 84: 304–9.
10 Muller AJ, DuHadaway JB, Donover PS, Sutanto-Ward E, Prendergast GC. Inhibition of indoleamine 2,3-dioxygenase, an immunoregulatory target of the cancer suppression gene *Bin1*, potentiates cancer chemotherapy. *Nat Med* 2005; 11: 312–9.
11 Hou DY, Muller AJ, Sharma MD *et al.* Inhibition of indoleamine 2,3-dioxygenase in dendritic cells by stereoisomers of 1-methyl-tryptophan correlates with antitumor responses. *Cancer Res* 2007; 67: 792–801.
12 Lob S, Konigsrainer A, Rammensee HG, Opelz G, Terness P. Inhibitors of indoleamine-2,3-dioxygenase for cancer therapy: can we see the wood for the trees? *Nat Rev Cancer* 2009; 9: 445–52.
13 Yang CS, Maliakal P, Meng X. Inhibition of carcinogenesis by tea. *Annu Rev Pharmacol Toxicol* 2002; 42: 25–54.
14 Yang CS, Wang X, Lu G, Picinich SC. Cancer prevention by tea: animal studies, molecular mechanisms and human relevance. *Nat Rev Cancer* 2009; 9: 429–39.
15 Shimizu M, Deguchi A, Lim JT, Moriwaki H, Kopelovich L, Weinstein IB. (−)-Epigallocatechin gallate and polyphenon E inhibit growth and activation of the epidermal growth factor receptor and human epidermal growth factor receptor-2 signaling pathways in human colon cancer cells. *Clin Cancer Res* 2005; 11: 2735–46.
16 Shimizu M, Deguchi A, Joe AK, McKoy JF, Moriwaki H, Weinstein IB. EGCG inhibits activation of HER3 and expression of cyclooxygenase-2 in human colon cancer cells. *J Exp Ther Oncol* 2005; 5: 69–78.
17 Shimizu M, Deguchi A, Hara Y, Moriwaki H, Weinstein IB. EGCG inhibits activation of the insulin-like growth factor-1 receptor in human colon cancer cells. *Biochem Biophys Res Commun* 2005; 334: 947–53.
18 Shirakami Y, Shimizu M, Tsurumi H, Hara Y, Tanaka T, Moriwaki H. EGCG and polyphenon E attenuate inflammation-related mouse colon carcinogenesis induced by AOM and DSS. *Mol Med Report* 2008; 1: 355–61.
19 Shimizu M, Shirakami Y, Sakai H *et al.* (−)-Epigallocatechin gallate suppresses azoxymethane-induced colonic premalignant lesions in male C57BL/KsJ–*db/db* mice. *Cancer Prev Res* 2008; 1: 298–304.
20 Pretlow TP, O'Riordan MA, Somich GA, Amini SB, Pretlow TG. Aberrant crypts correlate with tumor incidence in F344 rats treated with azoxymethane and phytate. *Carcinogenesis* 1992; 13: 1509–12.
21 Bird RP. Role of aberrant crypt foci in understanding the pathogenesis of colon cancer. *Cancer Lett* 1995; 93: 55–71.
22 Xiao H, Hao X, Simi B *et al.* Green tea polyphenols inhibit colorectal aberrant crypt foci (ACF) formation and prevent oncogenic changes in dysplastic ACF in azoxymethane-treated F344 rats. *Carcinogenesis* 2008; 29: 113–9.
23 Jeong YI, Jung ID, Lee JS, Lee CM, Lee JD, Park YM. (−)-Epigallocatechin gallate suppresses indoleamine 2,3-dioxygenase expression in murine dendritic cells: evidences for the COX-2 and STAT1 as potential targets. *Biochem Biophys Res Commun* 2007; 354: 1004–9.
24 Cheng CW, Shieh PC, Lin YC *et al.* Indoleamine 2,3-dioxygenase, an immunomodulatory protein, is suppressed by (−)-epigallocatechin-3-gallate via blocking of gamma-interferon-induced JAK-PKC-delta-STAT1 signaling in human oral cancer cells. *J Agric Food Chem* 2010; 58: 887–94.
25 Yamada Y, Yoshimi N, Hirose Y *et al.* Sequential analysis of morphological and biological properties of beta-catenin-accumulated crypts, provable premalignant lesions independent of aberrant crypt foci in rat colon carcinogenesis. *Cancer Res* 2001; 61: 1874–8.
26 Shimizu M, Sakai H, Shirakami Y *et al.* Preventive effects of (−)-epigallocatechin gallate on diethylnitrosamine-induced liver tumorigenesis in obese and diabetic C57BL/KsJ–*db/db* mice. *Cancer Prev Res* 2011; 4: 396–403.
27 Wang ZY, Agarwal R, Bickers DR, Mukhtar H. Protection against ultraviolet B radiation-induced photocarcinogenesis in hairless mice by green tea polyphenols. *Carcinogenesis* 1991; 12: 1527–30.
28 Moolenbeek C, Ruitenberg EJ. The "Swiss roll": a simple technique for histological studies of the rodent intestine. *Lab Anim* 1981; 15: 57–9.
29 Bird RP. Observation and quantification of aberrant crypts in the murine colon treated with a colon carcinogen: preliminary findings. *Cancer Lett* 1987; 37: 147–51.
30 Suzuki R, Kohno H, Yasui Y *et al.* Diet supplemented with citrus unshiu segment membrane suppresses chemically induced colonic preneoplastic lesions and fatty liver in male *db/db* mice. *Int J Cancer* 2007; 120: 252–8.
31 Sakai H, Yamada Y, Shimizu M, Saito K, Moriwaki H, Hara A. Genetic ablation of Tnfalpha demonstrates no detectable suppressive effect on inflammation-related mouse colon tumorigenesis. *Chem Biol Interact* 2010; 184: 423–30.
32 Hoshi M, Saito K, Hara A *et al.* The absence of IDO upregulates type I IFN production, resulting in suppression of viral replication in the retrovirus-infected mouse. *J Immunol* 2010; 185: 3305–12.
33 Suzuki Y, Suda T, Furuhashi K *et al.* Increased serum kynurenine/tryptophan ratio correlates with disease progression in lung cancer. *Lung Cancer* 2010; 67: 361–5.
34 Fujigaki S, Saito K, Sekikawa K *et al.* Lipopolysaccharide induction of indoleamine 2,3-dioxygenase is mediated dominantly by an IFN-gamma-independent mechanism. *Eur J Immunol* 2001; 31: 2313–8.
35 Fujigaki S, Saito K, Takemura M *et al.* The L-Tryptophan–L-kynurenine pathway metabolism accelerated by *Toxoplasma gondii* infection is abolished in gamma interferon-gene-deficient mice: cross-regulation between inducible nitric oxide synthase and indoleamine-2,3-dioxygenase. *Infect Immun* 2002; 70: 779–86.
36 Shimizu M, Shirakami Y, Iwasa J *et al.* Supplementation with branched-chain amino acids inhibits azoxymethane-induced colonic preneoplastic lesions in male C57BL/KsJ–*db/db* mice. *Clin Cancer Res* 2009; 15: 3068–75.
37 Yasuda Y, Shimizu M, Shirakami Y *et al.* Pitavastatin inhibits azoxymethane-induced colonic preneoplastic lesions in C57BL/KsJ–*db/db* obese mice. *Cancer Sci* 2010; 101: 1701–7.
38 Katz JB, Muller AJ, Prendergast GC. Indoleamine 2,3-dioxygenase in T-cell tolerance and tumoral immune escape. *Immunol Rev* 2008; 222: 206–21.
39 Dolusic E, Larrieu P, Moineaux L *et al.* Tryptophan 2,3-dioxygenase (TDO) inhibitors. 3-(2-(pyridyl)ethenyl)indoles as potential anticancer immunomodulators. *J Med Chem* 2011; 54: 5320–34.
40 Carlin JM, Borden EC, Sondel PM, Byrne GI. Interferon-induced indoleamine 2,3-dioxygenase activity in human mononuclear phagocytes. *J Leukoc Biol* 1989; 45: 29–34.
41 Takikawa O, Tagawa Y, Iwakura Y, Yoshida R, Truscott RJ. Interferon-gamma-dependent/independent expression of indoleamine 2,3-dioxygenase. Studies with interferon-gamma-knockout mice. *Adv Exp Med Biol* 1999; 467: 553–7.

42 von Bergwelt-Baildon MS, Popov A, Saric T *et al.* CD25 and indoleamine 2,3-dioxygenase are up-regulated by prostaglandin E_2 and expressed by tumor-associated dendritic cells *in vivo*: additional mechanisms of T-cell inhibition. *Blood* 2006; 108: 228–37.
43 Basu GD, Tinder TL, Bradley JM *et al.* Cyclooxygenase-2 inhibitor enhances the efficacy of a breast cancer vaccine: role of IDO. *J Immunol* 2006; 177: 2391–402.
44 Shimizu K, Kinouchi Shimizu N, Hakamata W, Unno K, Asai T, Oku N. Preventive effect of green tea catechins on experimental tumor metastasis in senescence-accelerated mice. *Biol Pharm Bull* 2010; 33: 117–21.
45 Chung KT, Gadupudi GS. Possible roles of excess tryptophan metabolites in cancer. *Environ Mol Mutagen* 2011; 52: 81–104.
46 Koblish HK, Hansbury MJ, Bowman KJ *et al.* Hydroxyamidine inhibitors of indoleamine-2,3-dioxygenase potently suppress systemic tryptophan catabolism and the growth of IDO-expressing tumors. *Mol Cancer Ther* 2010; 9: 489–98.
47 Munn DH, Sharma MD, Mellor AL. Ligation of B7-1/B7-2 by human $CD4^+$ T cells triggers indoleamine 2,3-dioxygenase activity in dendritic cells. *J Immunol* 2004; 172: 4100–10.
48 Raju J. Azoxymethane-induced rat aberrant crypt foci: relevance in studying chemoprevention of colon cancer. *World J Gastroenterol* 2008; 14: 6632–5.
49 Gupta AK, Pretlow TP, Schoen RE. Aberrant crypt foci: what we know and what we need to know. *Clin Gastroenterol Hepatol* 2007; 5: 526–33.
50 Mori H, Hata K, Yamada Y, Kuno T, Hara A. Significance and role of early-lesions in experimental colorectal carcinogenesis. *Chem Biol Interact* 2005; 155: 1–9.
51 Yasui Y, Suzuki R, Kohno H *et al.* 9*trans*,11*trans* conjugated linoleic acid inhibits the development of azoxymethane-induced colonic aberrant crypt foci in rats. *Nutr Cancer* 2007; 59: 82–91.
52 Eleftheriadis T, Antoniadi G, Liakopoulos V, Stefanidis I, Galaktidou G. Plasma indoleamine 2,3-dioxygenase concentration is increased in hemodialysis patients and may contribute to the pathogenesis of coronary heart disease. *Renal Fail* 2012; 34: 68–72.

doi: 10.1111/j.1349-7006.2012.02237.x

Therapeutics, Targets, and Chemical Biology

Cancer Research

Acyclic Retinoid Targets Platelet-Derived Growth Factor Signaling in the Prevention of Hepatic Fibrosis and Hepatocellular Carcinoma Development

Hikari Okada[1], Masao Honda[1,2], Jean S. Campbell[4], Yoshio Sakai[1], Taro Yamashita[1], Yuuki Takebuchi[1], Kazuhiro Hada[1], Takayoshi Shirasaki[1], Riuta Takabatake[1], Mikiko Nakamura[1], Hajime Sunagozaka[1], Takuji Tanaka[3], Nelson Fausto[4], and Shuichi Kaneko[1]

Abstract

Hepatocellular carcinoma (HCC) often develops in association with liver cirrhosis, and its high recurrence rate leads to poor patient prognosis. Although recent evidence suggests that peretinoin, a member of the acyclic retinoid family, may be an effective chemopreventive drug for HCC, published data about its effects on hepatic mesenchymal cells, such as stellate cells and endothelial cells, remain limited. Using a mouse model in which platelet-derived growth factor (PDGF)-C is overexpressed (*Pdgf-c Tg*), resulting in hepatic fibrosis, steatosis, and eventually, HCC development, we show that peretinoin significantly represses the development of hepatic fibrosis and tumors. Peretinoin inhibited the signaling pathways of fibrogenesis, angiogenesis, and Wnt/β-catenin in *Pdgf-c* transgenic mice. *In vitro*, peretinoin repressed the expression of PDGF receptors α/β in primary mouse hepatic stellate cells (HSC), hepatoma cells, fibroblasts, and endothelial cells. Peretinoin also inhibited PDGF-C–activated transformation of HSCs into myofibroblasts. Together, our findings show that PDGF signaling is a target of peretinoin in preventing the development of hepatic fibrosis and HCC. *Cancer Res; 72(17); 4459–71. ©2012 AACR.*

Introduction

Hepatocellular carcinoma (HCC) is one of the most common malignancies worldwide with a particularly poor patient outcome (1). It often develops as a result of chronic liver disease associated with hepatitis B or hepatitis C virus infection or with other etiologies such as long-term alcohol abuse, autoimmunity, and hemochromatosis (2–5). Despite the recent advances in antiviral therapy for hepatitis B or hepatitis C virus, these are insufficient to completely prevent the occurrence of HCC. Moreover, the recent increase in nonalcoholic fatty liver disease (NAFLD) associated with metabolic syndrome is a potential high-risk factor for the development of HCC (6).

HCC often develops during the advanced stages of liver fibrosis and is associated with deposits of extracellular matrix synthesized by activated stellate cells. During the course of chronic hepatitis, nonparenchymal cells, including Kupffer, endothelial, and activated stellate cells, release a variety of cytokines and growth factors. One of these growth factors is platelet-derived growth factor (PDGF), which is involved in fibrogenesis, angiogenesis, and tumorigenesis (7, 8). PDGF expression has been shown to be upregulated from the early stages of chronic hepatitis, suggesting its association with the development of fibrosis in chronic hepatitis C (CH-C; refs. 9 and 10). Overexpression of PDGF-C in mouse liver resulted in the progression of hepatic fibrosis, steatosis, and the development of HCC; this mouse model closely resembles the human HCC, which is frequently associated with hepatic fibrosis (7).

Peretinoin (generic name; code, NIK-333), developed by the Kowa Company, is an oral acyclic retinoid with a vitamin A–like structure, which targets the retinoid nuclear receptor. Oral administration of peretinoin was shown to significantly reduce the incidence of posttherapeutic HCC recurrence and improve the survival rates of patients in a clinical trial (11, 12). A large-scale clinical study including various countries is now planned to confirm its clinical efficacy.

Although peretinoin treatment can suppress HCC-derived cell line growth and inhibit experimental mouse or rat liver carcinogenesis (13, 14), the detailed mechanism of its effect has not been fully elucidated. Peretinoin has a high binding affinity to cellular retinoic acid-binding protein (15) and may interact with retinoic acid receptor-β and retinoid X receptor-α (16); however, the precise molecular targets for preventing HCC recurrence have not yet been elucidated.

Authors' Affiliations: [1]Department of Gastroenterology, Kanazawa University Graduate School of Medicine; [2]Department of Advanced Medical Technology, Kanazawa University Graduate School of Health Medicine; [3]Department of Oncologic Pathology, Kanazawa Medical University, Kanazawa, Japan; and [4]Department of Pathology, University of Washington School of Medicine, Seattle, Washington

Note: Supplementary data for this article are available at Cancer Research Online (http://cancerres.aacrjournals.org/).

Corresponding Author: Masao Honda, Department of Gastroenterology, Graduate School of Medicine, Kanazawa University, Takara-Machi 13-1, Kanazawa 920-8641, Japan. Phone: 81-76-265-2235; Fax: 81-76-234-4250; E-mail: mhonda@m-kanazawa.jp

doi: 10.1158/0008-5472.CAN-12-0028

In this study, we used PDGF-C transgenic (*Pdgf-c* Tg) mice to show that PDGF-C signaling is a possible target of peretinoin in the prevention of hepatic fibrosis, angiogenesis, and the development of HCC.

Materials and Methods

Chemicals

The acyclic retinoid peretinoin (generic name; code, NIK-333) [(2E,4E,6E,10E)-3,7,11,15-tetramethyl-2,4,6,10,14-hexadecapentaenoic acid, C20H30O2, molecular weight 302.46 g/mol] was supplied by Kowa Company.

Animal studies

The generation and characterization of *Pdgf-c Tg* have been described previously (7). Wild-type and *Pdgf-c Tg* mice on a C57BL/6J background were maintained in a pathogen-free animal facility under a standard 12-hour/12-hour light/dark cycle. After weaning at week 4, male mice were randomly divided into the following 3 groups: (1) *Pdgf-c Tg* or wild-type (WT) mice given a basal diet (CRF-1, Charles River Laboratories Japan), (2) *Pdgf-c Tg* or WT mice given a 0.03% peretinoin-containing diet, (3) *Pdgf-c Tg* or WT mice given a 0.06% peretinoin-containing diet. Control mice were normal male homozygotes. At week 20, mice were sacrificed to analyze the progression of hepatic fibrosis ($n = 15$ for each of the 3 groups). At week 48, mice were sacrificed to analyze the development of hepatic tumors ($n = 31$ for the basal diet group, $n = 37$ for the 0.03% peretinoin group, and $n = 17$ for the 0.06% peretinoin group). The incidence of hepatic tumors, maximum tumor size, and liver weight were evaluated. None of the treated WT mice given a diet of 0.03% peretinoin died, but death occurred in 5% of WT mice around after 36 weeks of age receiving a 0.06% peretinoin diet, probably because of its toxicity. In *Pdgf-c Tg* mice, death was observed at similar frequency as WT mice that received 0.06% peretinoin diet.

All animal experiments were carried out in accordance with Guidelines for the Care and Use of Laboratory Animals at the Takara-Machi Campus of Kanazawa University, Japan.

Cell culture

Human HCC cell lines Huh-7, HepG2, and HLE, the mouse fibroblast cell line NIH3T3, human umbilical vein endothelial cells (HUVEC), and human stellate cells Lx-2 (kindly provided by Dr. Scott Friedman, Mount Sinai School of Medicine, New York, NY) were maintained in Dulbecco's Modified Eagle Medium (DMEM; Gibco) supplemented with 10% FBS (Gibco), 1% L-glutamine (Gibco), and 1% penicillin/streptomycin (Gibco) in a humidified atmosphere of 5% CO_2 at 37°C. 1 to 5×10^4 cells were seeded in each well of a 12-well plate the day before serum starvation in serum-free DMEM for 8 hours. The culture medium was then replaced with serum-free medium containing peretinoin. After 24-hour incubation, cells were harvested for analysis.

Isolation and culture of mouse hepatic stellate cells

Hepatic stellate cells (HSC) were isolated from C57BL/6J mice and the effect of recombinant human PDGF-C and peretinoin on HSCs was evaluated *in vitro*. Pronase-collagenase liver digestion was used to isolate HSC from wild-type mice. All experiments were replicated at least twice. Freshly isolated HSCs suspended in culture medium were seeded in uncoated 24-well plates and incubated at 37°C in a humidified atmosphere of 5% CO_2 for 72 hours. Nonadherent cells were removed with a pipette and the culture medium was replaced with medium containing 80 ng/mL recombinant human PDGF-C (Abnova) with or without peretinoin or 9-*cis*-retinoic acid (9cRA; 5 or 10 μmol/L). Cells were harvested for analysis after 24-hour incubation.

Isolation of peripheral blood mononuclear cells

Peripheral blood mononuclear cells were harvested and labeled with FITC-conjugate CD34 (Cell Lab) and R-Phycoerythrin (PE)-conjugated CD31 antibodies (Cell Lab) for 30 minutes at 4°C. After washing with 1 mL PBS, CD31 and CD34 surface expression was measured with a FACSCalibur flow cytometer (BD Biosciences). All flow cytometric data were analyzed using FlowJo software (Tree Star).

Gene expression profiling

Gene expression profiling in mouse liver was evaluated using the GeneChip Mouse Genome 430 2.0 Array (Affymetrix). Liver tissue from WT, *Pdgf-c Tg*, and *Pdgf-c Tg* with 0.06% peretinoin mice all at weeks 20 and 48 was obtained and a total of 34 chip assays were conducted as described previously (17). Expression data have been deposited in the Gene Expression Omnibus (GEO; NCBI Accession; GSE31431).

Pathway analysis was conducted using MetaCore (GeneGo). Functional ontology enrichment analysis was conducted to compare the Gene Ontology (GO) process distribution of differentially expressed genes ($P < 0.01$; refs. 10 and 17). Direct interactions among differentially expressed genes between *Pdgf-c Tg* mice with or without peretinoin administration were examined as reported previously (10). Each connection represents a direct, experimentally confirmed, physical interaction (MetaCore).

Histopathology and immunohistochemical staining

Mouse liver tissues were fixed in 10% formalin and stained with hematoxylin and eosin. The liver neoplasms (HCC and liver cell adenoma) were diagnosed according to previously described criteria (18, 19). Hepatic fibrosis was evaluated by Azan staining. Percentages of fibrous areas were calculated microscopically using an image analysis system (BIOREVO BZ-9000: KEYENCE Japan). Immunohistochemical (IHC) staining was conducted by an immunoperoxidase technique with an Envision kit (DAKO). Primary antibodies used were: rabbit polyclonal PDGFR-α (1:100 dilution), PDGFR-β (1:100 dilution), VEGFR1 (1:100 dilution), desmin (1:100 dilution), β-catenin (1:200 dilution), and mouse monoclonal cyclin D1 (1:400 dilution; all from Cell Signaling Technology); collagen 1 (1:100 dilution), collagen 4 (1:100 dilution), CD31 (1:100 dilution), and CD34 (1:100 dilution; all from Abcam, Cambridge, MA); and Tie-2 (1:80 dilution) and Myc (1:100 dilution; both from Santa Cruz Biotechnology).

Quantitative real-time detection PCR

Total RNA was isolated from frozen liver tissue samples using a GenElute Mammalian Total RNA Miniprep Kit (Sigma-Aldrich) according to the manufacturer's protocol. cDNA was synthesized from 100 ng total RNA using a high-capacity cDNA reverse transcription kit (Applied Biosystems) then mixed with the TaqMan Universal Master Mix (Applied Biosystems) and each TaqMan probe. TaqMan probes used were PDGFR-α/β, VEGFR1/2, α-SMA, collagen 1/4, β-catenin, CyclinD1, and Myc (Applied Biosystems). Relative expression levels were calculated after normalization to glyceraldehyde-3-phosphate dehydrogenase (GAPDH).

Western blotting

Western blotting was conducted as described previously (20). Whole-cell lysates from mouse liver were prepared and lysed by CelLytic MT cell lysis reagent (Sigma-Aldrich) containing Complete Mini EDTA-free Protease Inhibitor cocktail tablets (Roche). Cytoplasmic and nuclear protein extracts were prepared using the NE-PER nuclear extraction reagent kit (Pierce Biotechnology). Primary antibodies used were PDGFR-α (1:1,000 dilution), PDGFR-β (1:1,000 dilution), VEGFR2 (1:1,000 dilution), p44/42 MAPK (1:1,000 dilution), total AKT (1:1,000 dilution), p-p44/42 MAPK (1:1,000 dilution), p-AKT (Ser473; 1:1,000 dilution), p-AKT (Thr308; 1:1,000 dilution), β-catenin (1:2,000 dilution), cyclin D1 (1:400 dilution), and lamin A/C (1:1,000 dilution; all Cell Signaling Technology); α-SMA (1:200 dilution; DAKO); 4-HNE (1:200 dilution; NOF); and GAPDH (1:1,000 dilution) and Myc (1:1,000 dilution; both Santa Cruz).

Statistical analysis

Results are expressed as mean ± SD. Significance was tested by 1-way analysis of variance with Bonferroni's method, and differences were considered statistically significant at $P < 0.05$.

Results

Peretinoin prevented the development of hepatic fibrosis in Pdgf-c Tg

To evaluate the HCC chemopreventive effects of peretinoin, we used a mouse model of *Pdgf-c Tg* in which PDGF-C is expressed under the control of the albumin promoter (7). Experimental mice were male mice expressing the PDGF-C transgene (*Pdgf-c Tg*); whereas male mice not expressing the transgene were considered WT. After weaning at week 4, *Pdgf-c Tg* or nontransgenic WT mice were fed a basal diet or a diet containing 0.03% or 0.06% peretinoin. At week 20, mice were sacrificed to analyze the progression of hepatic fibrosis. At week 48, mice were sacrificed to analyze the development of hepatic tumors (Fig. 1A). At week 20, Azan staining showed that predominant pericellular fibrosis had developed in *Pdgf-c Tg* mice (Fig. 1B). Densitometric analysis showed a significant dose-dependent reduction in the size of the fibrotic area in mice that received a diet containing peretinoin at both weeks 20 and 48 (Fig. 1C). Peretinoin therefore efficiently repressed the development of hepatic fibrosis in *Pdgf-c Tg* mice.

The expression of fibrosis-related genes in *Pdgf-c Tg* mice was evaluated by IHC staining, quantitative real-time detection PCR (RTD-PCR), and Western blotting. The expression of PDGFR-α and PDGFR-β, essential receptors for intracellular PDGF-C signaling, was upregulated mainly in the intracellular or portal area in *Pdgf-c Tg* mice livers (Fig. 2), but was significantly repressed by peretinoin after weaning at week 4. Similarly, the expression of collagen 1, collagen 4, and desmin was significantly upregulated in *Pdgf-c Tg* mice, but repressed by peretinoin (Fig. 2 and Supplementary Fig. S1A).

RTD-PCR results confirmed that these genes were substantially upregulated in *Pdgf-c Tg* mice and significantly repressed by both 0.03% and 0.06% peretinoin (Fig. 3A). Western blotting showed that the expression of phosphorylated extracellular signal-regulated kinase (p-ERK) 1/2 and cyclin D1, representative markers of the cell proliferation signaling pathway, was upregulated in *Pdgf-c Tg* mice, and repressed by peretinoin (Fig. 3B). Thus, peretinoin could partially but significantly prevent the development of hepatic fibrosis in *Pdgf-c Tg* mice during the study observation period of 48 weeks.

Peretinoin prevented the development of HCC in Pdgf-c Tg mice

At week 48, *Pdgf-c Tg* mice developed hepatic tumors with an incidence of 90% (Fig. 4A). Histologic assessment of these tumors verified that 54% (15/28) were adenomas and 46% (13/28) were HCC (Fig. 4A and C and Supplementary Fig. S2; ref. 21). Peretinoin (0.03%) dose-dependently repressed the incidence of hepatic tumors to 53% (19/36) and to 29% (5/17) at 0.06%. Correlating with tumor incidence, maximum tumor size and liver weight were also significantly repressed by peretinoin (Fig. 4B). Thus, peretinoin repressed the development of hepatic tumors in *Pdgf-c Tg* mice.

Serial gene expression profiling in the liver of Pdgf-c Tg mice that developed hepatic fibrosis and tumors

To examine which signaling pathways were altered during the progression of hepatic fibrosis and tumor development, we analyzed gene expression profiling in the liver of *Pdgf-c Tg* mice using Affymetrix gene chips. By filtering criteria for $P < 0.001$ and more than 2-fold differences, 538 genes were selected as differentially expressed. One-way hierarchical clustering analysis of differentially expressed genes is shown in Supplementary Fig. S3.

Of the 3 main clusters, 2 were upregulated (clusters A and B) and 1 was downregulated (cluster C). Cluster A consisted of immune-related [chemokine (C-C motif) receptor (CCR)4, CCR2, toll-like receptor (TLR)3 and TLR4], apoptosis-related [caspase (CASP)1 and CASP9], angiogenesis- and/or growth factor–related (PDGF-C, VEGF-C, osteopontin, HGF), oncogene-related [v-ets erythroblastosis virus E26 oncogene homologue (Ets)1, Ets2, CD44, N-myc downstream-regulated (NDRG)1], and fibrosis-related (tubulin) genes. The expression of cluster A genes was further upregulated in tumors at week

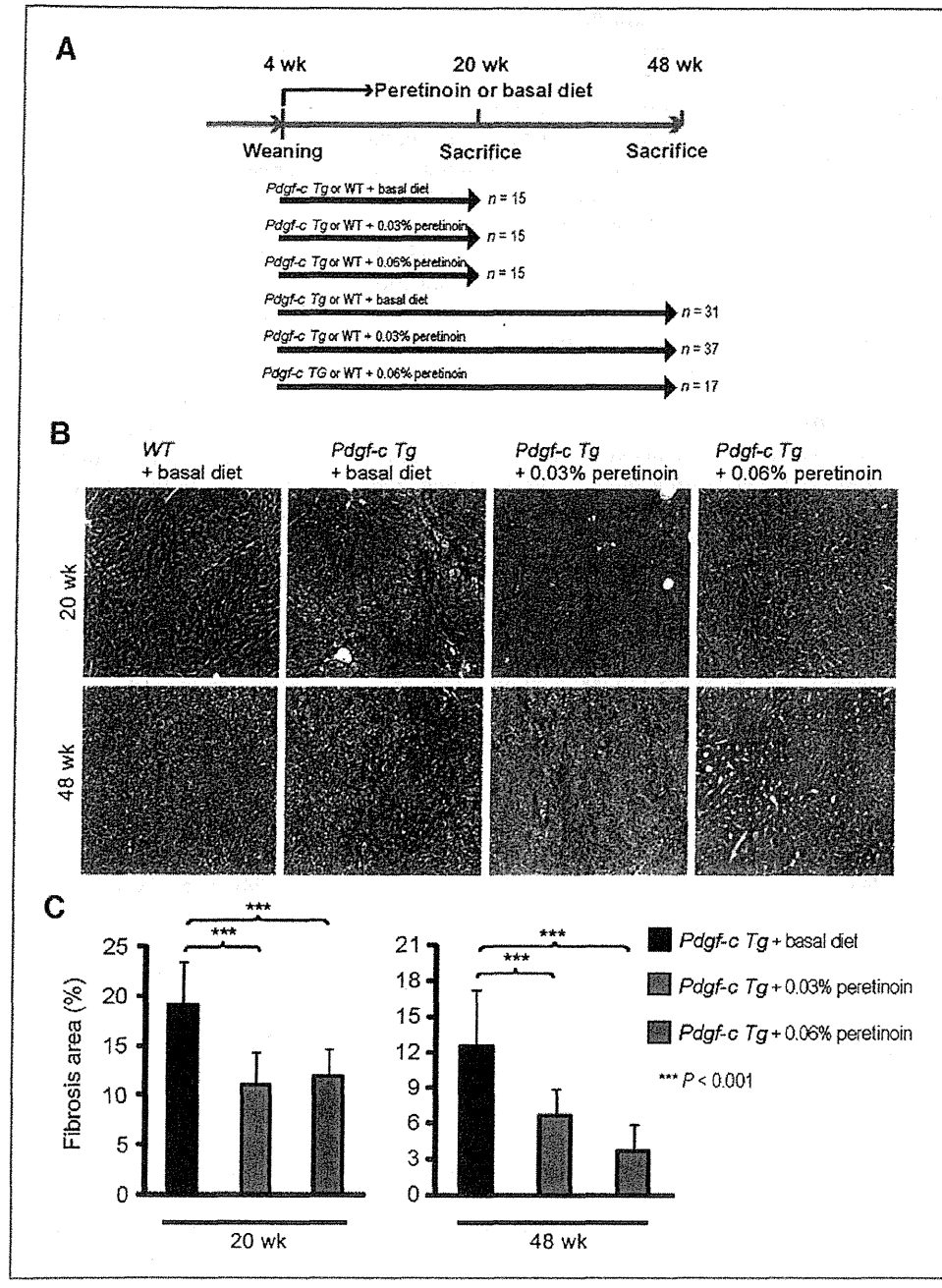

Figure 1. A, feeding schedule of Pdgf-c Tg and WT mice. After weaning, male mice were randomly divided into 3 groups: (i) Pdgf-c Tg or WT mice receiving basal diet, (ii) Pdgf-c Tg or WT mice receiving 0.03% peretinoin-containing diet, and (iii) Pdgf-c Tg or WT mice receiving 0.06% peretinoin-containing diet. B, Azan staining of WT or Pdgf-c Tg mouse livers fed with different diets at 20 weeks and 48 weeks. C, densitometric analysis of Pdgf-c Tg mouse liver fibrotic areas at 20 weeks (n = 15) and 48 weeks (n = 15).

48. Cluster B consisted mainly of connective tissue- and/or fibrosis-related [vascular cell adhesion molecule (VCAM)1, collagen I, III, IV, V, VI, integrin, decorin, TGF-βRII, PDGFR-α, and PDGFR-β] genes, the expression of which declined slightly at week 48. In contrast, cluster C, containing differentiation and liver function related genes [cytochrome P450, family 2, subfamily c (CYP2C)], were downregulated during the course of hepatic fibrosis and tumor development (Supplementary Fig. S4). Cluster C included xenobiotic- and metabolic process–related genes, which are potential targets of peretinoin. Peretinoin treatment prevented hepatic fibrosis and it preserved liver function. In addition, peretinoin might induce its target genes. Thus, peretinoin reduced the expression of upregulated genes (clusters A and B) and restored the expression of downregulated genes (cluster C) at both weeks 20 and 48 (Supplementary Figs. S3 and S4).

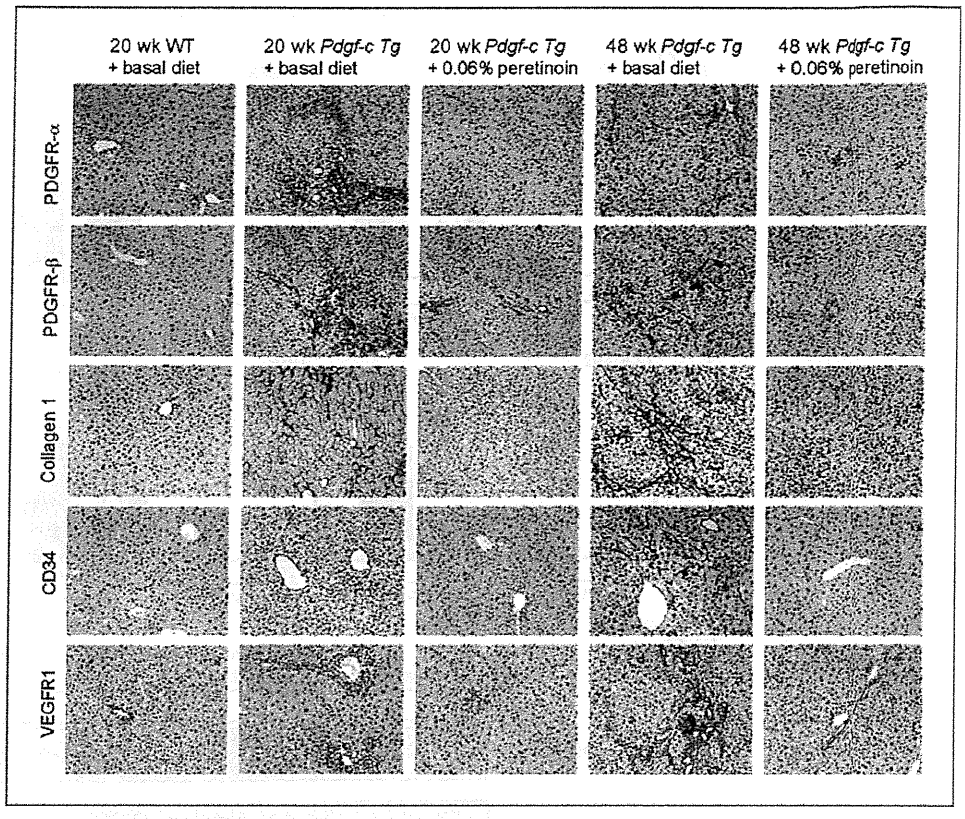

Figure 2. IHC staining of PDGFR-α, PDGFR-β, collagen 1, CD34, and VEGFR1 expression in Pdgf-c Tg or WT mouse livers fed a basal diet or 0.06% peretinoin.

To examine the molecular network consisting of differentially expressed genes in *Pdgf-c Tg* mice with or without peretinoin administration, the direct interactions of 513 genes were analyzed by MetaCore (i.e., 413 genes were downregulated and 100 genes were upregulated in *Pdgf-c Tg* mice treated with peretinoin compared with untreated mice; $P < 0.002$). A core gene network consisting of 41 genes was obtained (Supplementary Fig. S5) including interactions between representative growth factors, receptors (PDGFR and TGFβR), and transcriptional factors. Of these genes, the transcriptional factors Sp1 and Ap1 seem to be key regulators in the network (Supplementary Fig. S5).

Peretinoin inhibits PDGFR *in vitro*

Gene expression profiling landscaped the dynamic changes of signaling pathways in *Pdgf-c Tg* mice. To determine the effects of peretinoin *in vitro*, primary HSCs from normal C57BL/6J mice were stimulated by PDGF-C (Fig. 5) to induce the expression of PDGFR-α, PDGFR-β, alpha smooth muscle actin (α-SMA), and collagen 1a2; activated HSCs thus transformed into myofibroblasts (Fig. 5A and B). Peretinoin significantly reduced the expression of these genes and inhibited HSC activation.

We next evaluated the effects of peretinoin on human hepatoma cell lines (Huh-7, HepG2, and HLE), mouse embryonic fibroblast cells (NIH3T3), HUVECs, and Lx-2 (ref. 22; Supplementary Fig. S6A). Experimental conditions were optimized so that more than 90% of cells were variable at 20 μmol/L peretinoin, as determined by an MTS cell proliferation assay (data not shown). Peretinoin dose-dependently inhibited the expression of PDGFR-α and PDGFR-β in Huh-7, HepG2, HLE, NIH3T3, HUVEC, and Lx-2 cells, whereas no obvious expression of PDGFR-α was observed in HepG2 cells and HUVECs (Supplementary Fig. S6A). Peretinoin also inhibited VEGFR2 expression in HUVEC. These results were confirmed by RTD-PCR (data not shown). Correlating with these results, the expression of phosphorylated serine/threonine kinase AKT (p-AKT) and p-ERK1/2, downstream signaling molecules of PDGFR-α, PDGFR-β, and VEGFR2, was also dose-dependently repressed. The expression of collagen 1a2 was significantly repressed by peretinoin in Lx-2, HLE, and Huh-7 cells (Supplementary Fig. S6B). These results suggest that peretinoin may inhibit hepatic fibrosis, angiogenesis, and tumor growth through reduction of the PDGF and VEGF signaling pathway.

We examined the expression of 2 key regulators in peretinoin signaling, Sp1 and Ap1, in Huh-7 cells. Interestingly, the expression of Sp1 was decreased, which correlates with that of PDGFR-α, whereas expression of phosphorylated c-Jun (p-c-Jun) was increased in Huh-7 cells (Supplementary Fig. S6C). Therefore, peretinoin seems to repress the expression of PDGFR, partially through the inhibition of Sp1.

Peretinoin inhibits hepatic angiogenesis in Pdgf-c Tg mice

The effect of peretinoin on liver angiogenesis in *Pdgf-c Tg* mice was further analyzed. IHC staining of *Pdgf-c Tg* mouse

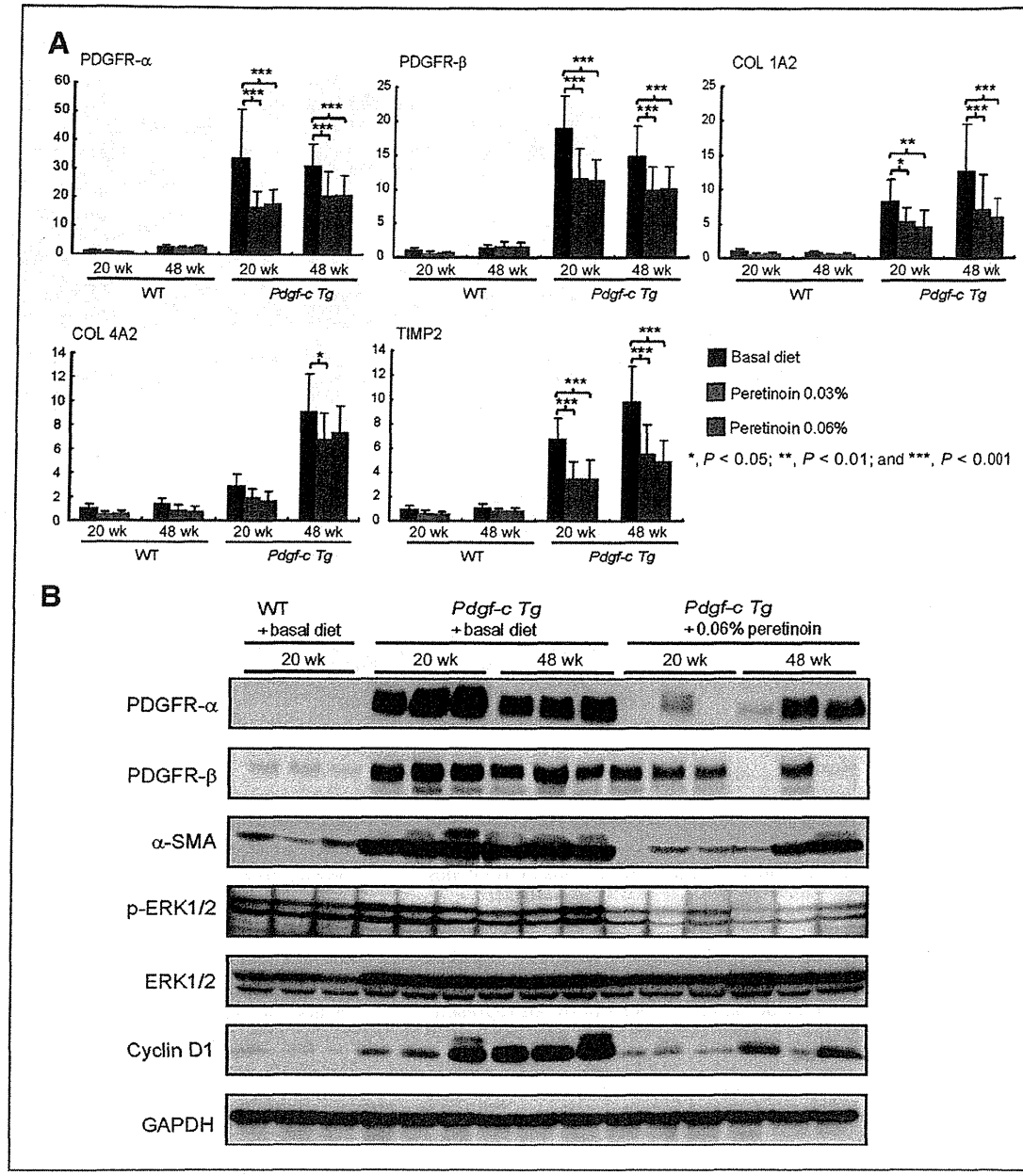

Figure 3. A, RTD-PCR analysis of PDGFR-α, PDGFR-β, collagen (COL) 1a2, collagen 4 a2, and TIMP2 expression in Pdgf-c Tg (n = 5) or WT mouse livers (n = 15). B, Western blotting of PDGFR-α, PDGFR-β, α-SMA, p-ERK, ERK, cyclin D1, and GAPDH expression in PDGF-C Tg or WT mouse livers fed a basal diet or 0.06% peretinoin at 20 or 48 weeks (n = 3).

livers at weeks 20 and 48 revealed overexpression of the endothelial markers CD31 and CD34 and the endothelial growth factors VEGFR1 and endothelium-specific receptor tyrosine kinase 2 (Tie2) in the mesenchymal region (Fig. 6 and Supplementary Fig. S1A). This expression was significantly repressed by peretinoin as determined by the densitometric area (Supplemental Fig. S1B). RTD-PCR results revealed significant upregulation of VEGFR1 (Flt-1) in *Pdgf-c Tg* mice compared with WT mice at both weeks 20 and 48, whereas the expression of VEGFR2 (Flk-1) and Tie2 was only upregulated at week 48. The expression of these genes was significantly repressed by peretinoin (Fig. 6A). Western blotting confirmed the upregulation of CD31 and VEGFR1 (Flk-1) at week 48 (Fig. 6B). In addition, p-AKT (Thr 308 and Ser 473) and 4-hydroxy-2-nonenal (4-HNE), an oxidative stress marker, were upregulated in *Pdgf-c Tg* mice and repressed by peretinoin (Fig. 6B).

We also assessed circulating endothelial cells (CEC), a useful biomarker for angiogenesis in the blood, and found that the $CD31^+/CD34^+$ CEC population was significantly upregulated in *Pdgf-c Tg* mice at week 48 but significantly repressed by peretinoin (Fig. 6C and D). Thus, peretinoin

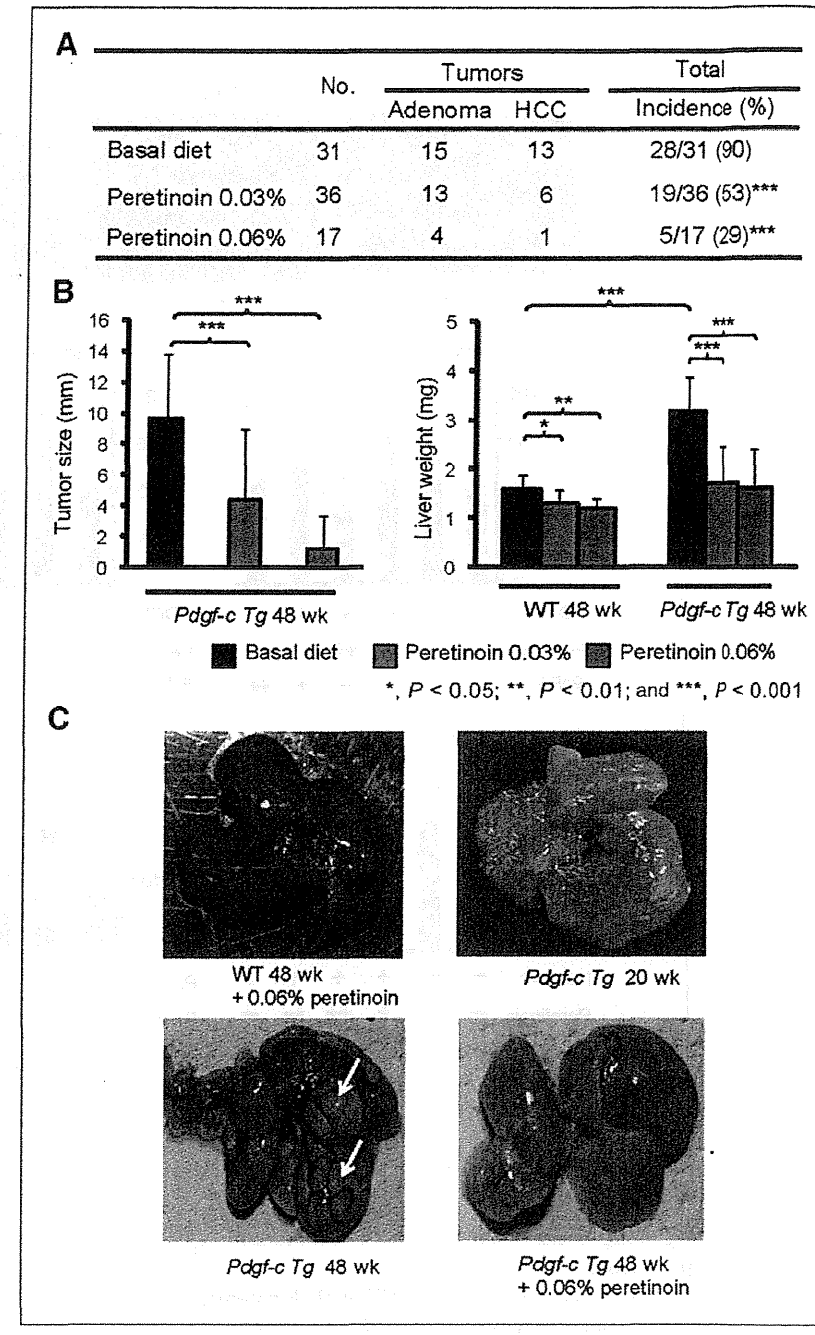

Figure 4. A, incidence of hepatic tumors (adenoma or HCC) in Pdgf-c Tg mouse livers fed with different diets. B, tumor sizes and liver weights of Pdgf-c Tg and WT mice fed with basal diet (n = 31 for Pdgf-c Tg, n = 15 for WT mice) or 0.03% (n = 36 for Pdgf-c Tg, n = 15 for WT mice) and 0.06% (n = 17 for Pdgf-c Tg, n = 15 for WT mice) peretinoin at 48 weeks. C, macroscopic findings of Pdgf-c Tg or WT mouse livers. No obvious change was observed in the liver of WT mice fed with 0.06% peretinoin for 48 weeks (top left). Fibrosis and steatosis were observed in the liver of Pdgf-c Tg mice fed a basal diet for 20 weeks (top right). Multiple tumors developed (white arrows) in the liver of Pdgf-c Tg mice fed a basal diet for 48 weeks (bottom left). Suppression of tumor development in the liver of Pdgf-c Tg mice fed a 0.06% peretinoin diet for 48 weeks (bottom right).

seems to inhibit angiogenesis in the liver of *Pdgf-c Tg* mice, which might prevent the development of hepatic tumors.

Peretinoin inhibits canonical Wnt/β-catenin signaling in Pdgf-c Tg mice

The activation of the Wnt/β-catenin signaling pathway is seen in 17% to 40% of patients with primary HCC (23, 24). Moreover, recent reports suggested an interaction between PDGF signaling and Wnt/β-catenin signaling (25–27). We evaluated Wnt/β-catenin signaling in *Pdgf-c Tg* mice and showed by IHC staining that β-catenin was overexpressed in the submembrane at week 48 (Fig. 7A). Peretinoin significantly reduced this expression (Fig. 7A and B), and Western blotting revealed that accumulation of β-catenin in the nuclear fraction of liver tumor tissues was more preferentially repressed by peretinoin than in the cytoplasmic fraction, although expression was repressed in both fractions (Fig. 7C). Wnt ligand (Wnt5a) and frizzled receptor (Fzd1) expression was significantly upregulated in hepatic tumors compared with normal liver (Fig. 7D). These results together suggest that canonical Wnt/β-catenin

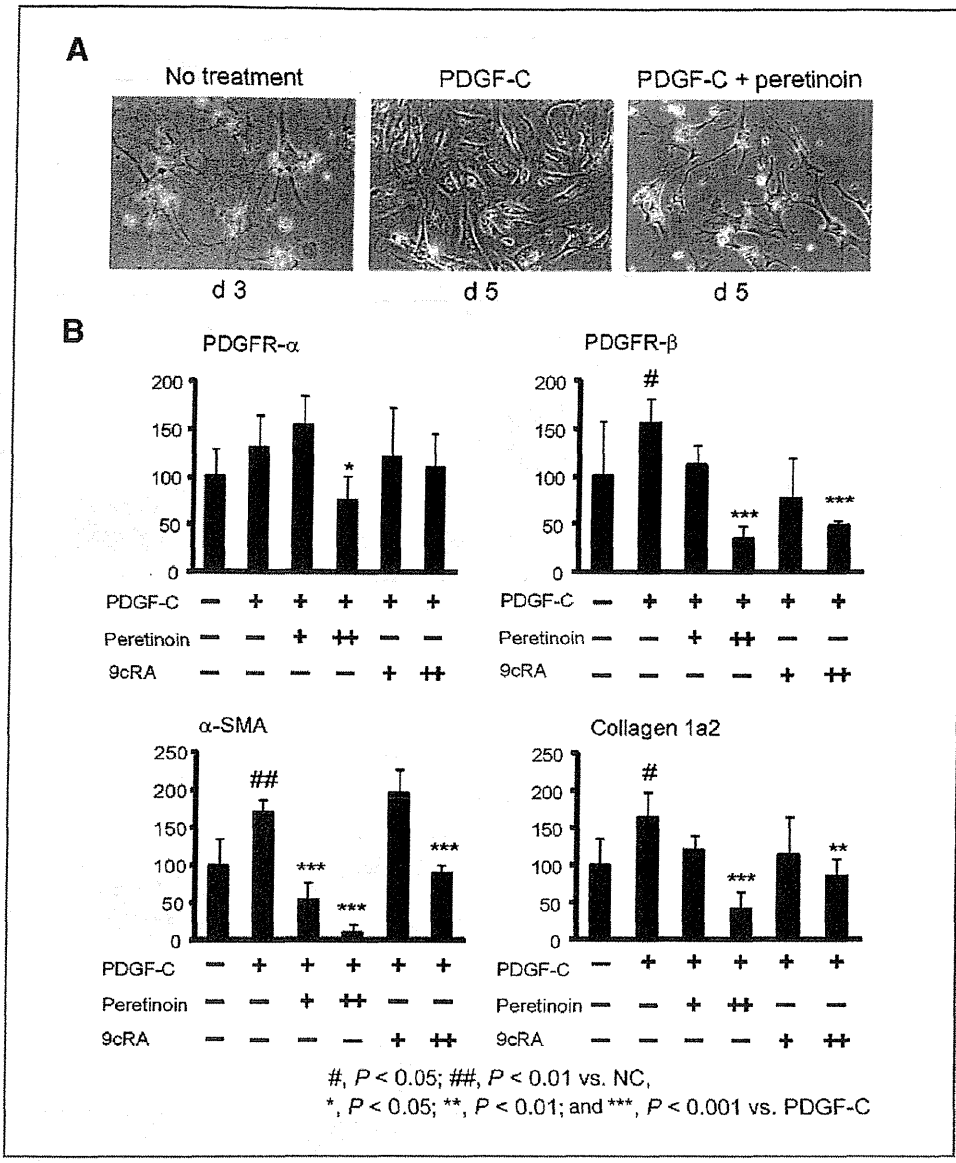

Figure 5. A, microscopic view of freshly isolated primary mouse HSCs after PDGF-C transformation into myo□broblasts (left). Peretinoin inhibited the transformation of HSCs by PDGF-C. B, RTD-PCR analysis of PDGFR-α, PDGFR-β, α-SMA, and collagen 1a2 expression in HSCs treated with or without PDGF-C, peretinoin, and 9cRA (n = 4). PDGF-C (+), 80 ng/mL; peretinoin (+), 5 μmol/L; (++), 10 μmol/L; 9cRA (+), 5 μmol/L; (++), 10 μmol/L. NC, no control.

signaling is activated in hepatic tumors and repressed by peretinoin.

Growth factors such as PDGF or HGF potentially activate Wnt/β-catenin signaling (26, 28), which promotes cancer progression and metastasis. We evaluated whether such growth factor signaling could be repressed by peretinoin in hepatic tumors. The expression of c-myc, β-catenin, Tie2, Fit-1, and Flk-1 were significantly upregulated from 1.5- to 4-fold in hepatic tumors compared with normal liver, and this expression was significantly repressed by peretinoin. Similarly, the expression of PDGFR-α, PDGFR-β, collagen 1a2, collagen 4a2, tissue inhibitor of metalloproteinase 2 (TIMP2), and cyclin D1 was substantially upregulated from 5- to 15-fold in hepatic tumors, and significantly repressed by peretinoin (Fig. 7D). Thus, growth factor signaling as well as canonical Wnt/β-catenin signaling in hepatic tumors seems to be repressed by peretinoin. These results explain the inhibitory effect of peretinoin in the development of HCC in *Pdgf-c Tg* mice.

Discussion

HCC often develops in association with liver cirrhosis and its high recurrence rate leads to poor patient prognosis. Indeed, the 10-year recurrence-free survival rate after liver resection for HCC with curative intent was shown to be only 20% (29). Therefore, there is a pressing need to develop effective preventive therapy for HCC recurrence to improve its prognosis.

Peretinoin, a member of the acyclic retinoid family, is expected to be an effective chemopreventive drug for HCC (11, 12, 30) as shown by a previous phase II/III trial in which 600 mg peretinoin per day in the Child-Pugh A subgroup reduced the risk of HCC recurrence or death by 40% [HR = 0.60 (95% CI, 0.40–0.89); ref. 31]. However, further clinical

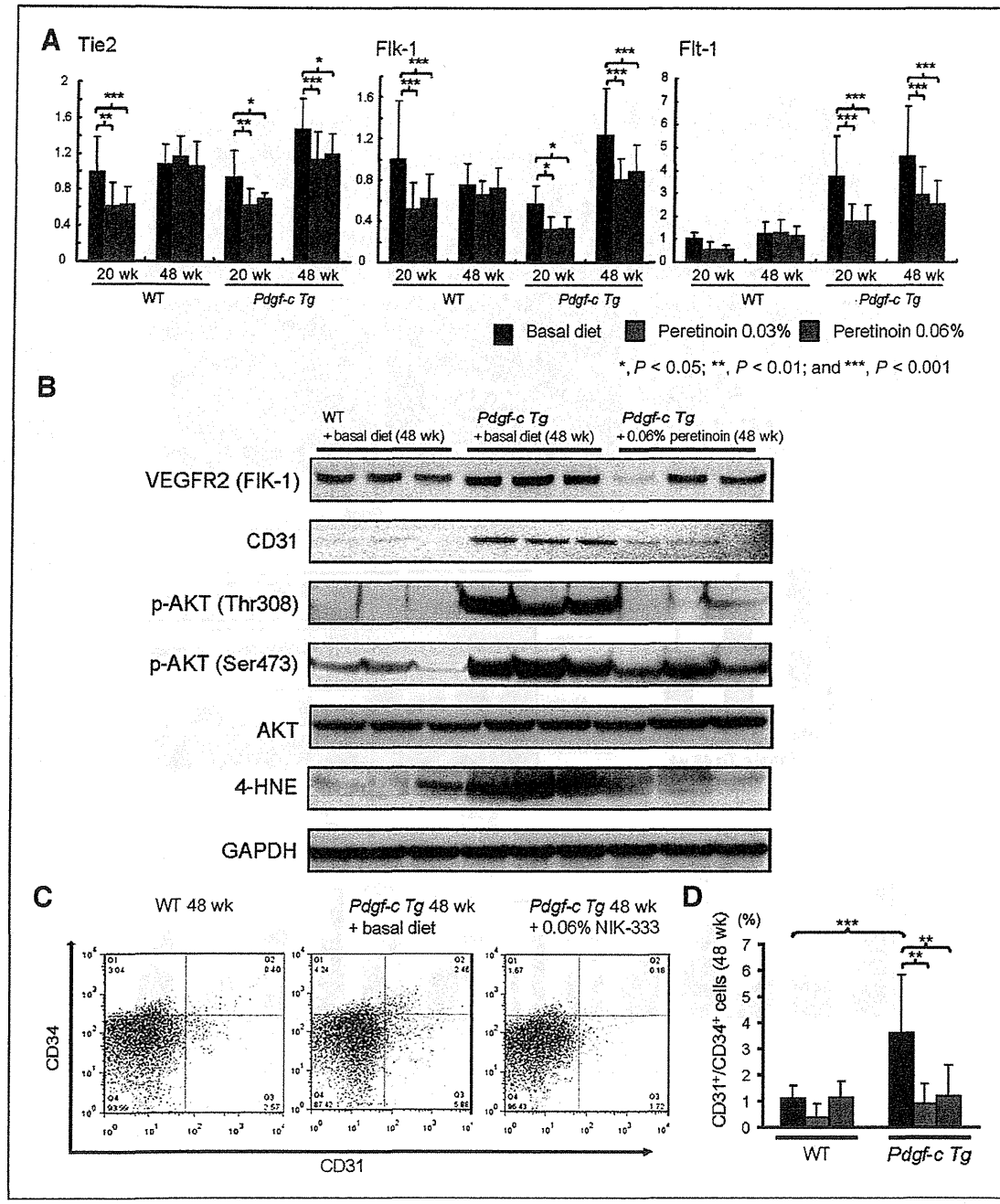

Figure 6. A, RTD-PCR analysis of Tie2, Flk-1, and Flt-1 expression in the liver of Pdgf-c Tg and WT mice fed with different diets (n = 15). B, Western blotting of Flk-1, CD31, p-AKT (Thr 308, Ser473), AKT, 4-HNE, and GAPDH expression in the liver of Pdgf-c Tg or WT mice fed a basal diet or 0.06% peretinoin at 48 weeks (n = 3). C, fluorescence-activated cell-sorting analysis of CD31- and CD34-positive CEC in blood of Pdgf-c Tg or WT mice fed a basal diet or 0.06% peretinoin at 48 weeks. D, frequency of CD31- and CD34-positive CEC in blood of Pdgf-c Tg or WT mice fed a basal diet or 0.06% peretinoin at 48 weeks (n = 10).

studies are needed to confirm the clinical efficacy of peretinoin, and a large scale study involving several countries is currently being planned.

During the course of chronic hepatitis, nonparenchymal cells including Kupffer, endothelial and activated stellate cells release a variety of cytokines and growth factors that might accelerate hepatocarcinogenesis. Although peretinoin has been shown to suppress the growth of HCC-derived cells by inducing apoptosis and differentiation (32–35), increasing p21 and reducing cyclin D1 (13), limited data have been published about its effects on hepatic mesenchymal cells such as stellate cells and endothelial cells (14).

In parallel with a phase II/III trial, we conducted a pharmacokinetics study of peretinoin focusing on 12

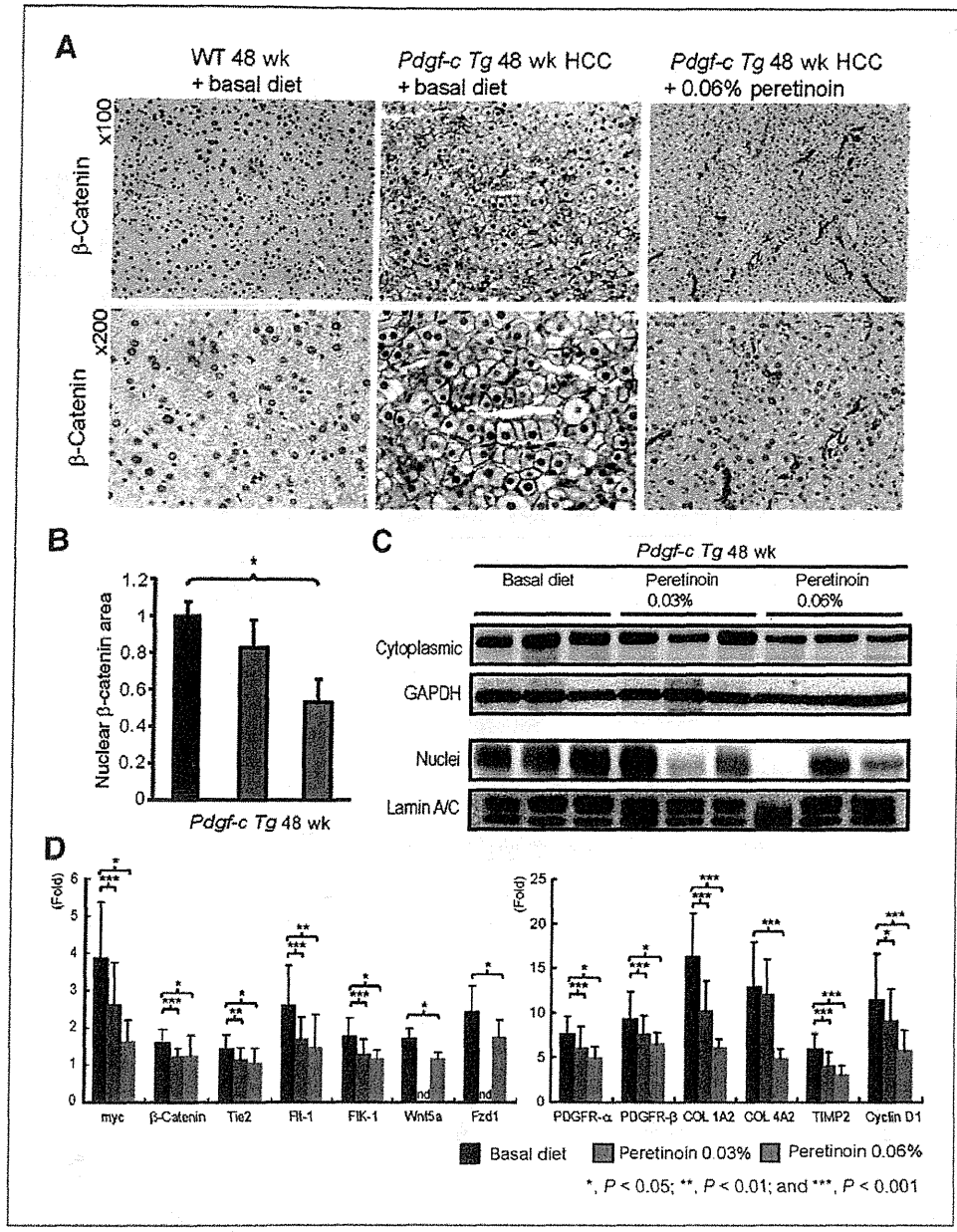

Figure 7. A, IHC staining of β-catenin expression in HCC tissues of Pdgf-c Tg mice fed a basal diet or 0.06% peretinoin at 48 weeks. B, densitometric analysis of β-catenin expression in the liver of Pdgf-c Tg mice fed with different diets (n = 15 for basal diet, n = 15 for 0.03% peretinoin, n = 5 for 0.06% peretinoin). C, Western blotting of β-catenin expression in cytoplasmic and nuclear fractions of Pdgf-c Tg mouse livers fed with different diets. GAPDH was used to standardize cytoplasmic protein and lamin A/C to standardize nuclear protein (n = 3). D, RTD-PCR analysis of myc, β-catenin, Tie2, Flt-1, Flk-1, Wnt5a, Fzd1, PDGFR-α, PDGFR-β, collagen (COL) 1a2, collagen 4a2, TIMP2, and cyclin D1 expression in HCC tissues of Pdgf-c Tg mice fed with different diets (n = 15 for basal diet, n = 15 for 0.03% peretinoin, n = 5 for 0.06% peretinoin). Relative fold expressions compared with WT mice are shown.

patients with CH-C and HCC to monitor the biological behavior of peretinoin in the liver. Gene expression profiling during peretinoin administration revealed that HCC recurrence within 2 years could be predicted and that PDGF-C expression was one of the strongest predictors. In addition, other genes related to angiogenesis, cancer stem cell and tumor progression were downregulated, whereas expression of genes related to hepatocyte differentiation and tumor suppression was upregulated by peretinoin (data not shown). Moreover, a recent report revealed the emerging significance of PDGF-C–mediated angiogenic and tumorigenic properties (7, 8, 36). In this study, we therefore used the mouse model of *Pdgf-c Tg*, which displays the phenotypes of hepatic fibrosis, steatosis, and HCC development that resemble human HCC arising from chronic hepatitis usually associated with advanced hepatic fibrosis.

We showed that peretinoin effectively inhibits the progression of hepatic fibrosis and tumors in *Pdgf-c Tg* mice (Figs. 1 and 4). Affymetrix gene chips analysis revealed dynamic changes in hepatic gene expression (Supplementary Fig. S3), which were confirmed by IHC staining, RTD-PCR and Western blotting. Pathway analysis of differentially expressed genes suggested that the transcriptional regulators Sp1 and Ap1 are key regulators in the peretinoin inhibition of hepatic fibrosis and tumor development in *Pdgf-c Tg* mice (Supplementary Fig. S5).

We clearly showed that peretinoin inhibited PDGF signaling through the inhibition of PDGFRs (Figs. 2 and 3). In

addition, we showed that PDGFR repression by peretinoin inhibited primary stellate cell activation (Fig. 5). Interestingly, this inhibitory effect was more pronounced than the effects of 9cRA (Fig. 5B). Normal mouse and human hepatocytes neither express PDGF receptors (J.S. Campbell and N. Fausto, unpublished data), nor proliferate in response to treatment with PDGF ligands (7). However, peretinoin inhibited the expression of PDGFRs, collagens, and their downstream signaling molecules in cell lines of hepatoma (Huh-7, HepG2, and HLE), fibroblast (NIH3T3), endothelial cells (HUVEC), and stellate cells (Lx-2; Supplementary Fig. S6). Furthermore, Sp1 but not Ap1, might be involved in the repression of PDGFR-α in Huh-7 cells (Supplementary Fig. 6C). The overexpression of Sp1-activated PDGFR-α promoter activity, whereas siRNA knockdown of Sp1 repressed PDGFR-α promoter activity in Huh-7 cells (data not shown). Therefore, this seems to confirm that Sp1 is involved in the regulation of PDGFR, as reported previously (37, 38), although these findings should be further investigated in different cell lines. A recent report showed the involvement of transglutaminase 2, caspase3, and Sp1 in peretinoin signaling (35).

Peretinoin was shown to inhibit angiogenesis in the liver of *Pdgf-c Tg* mice in this study, as shown by the decreased expression of VEGFR1/2 and Tie 2 (Figs. 2 and 6 and Supplementary Fig. S1). Moreover, peretinoin inhibited the number of $CD31^+$ and $CD34^+$ endothelial cells (CEC) in the blood and liver (Fig. 6C and D), while also inhibiting the expression of EGFR, c-kit, PDGFRs, and VEGFR1/2 in *Pdgf-c Tg* mice (data not shown). We also showed that peretinoin inhibited the expression of multiple growth factors such as HGF, IGF, VEGF, PDGF, and HDGF, which were upregulated from 3- to 10-fold in *Pdgf-c Tg* mice (Supplementary Fig. S3). These activities collectively might contribute to the antitumor effect of peretinoin in *Pdgf-c Tg* mice. The inhibition of both PDGFRs and VEGFR signaling by peretinoin was previously shown to have a significant effect on tumor growth (36), and we confirmed herein that peretinoin inhibited the expression of VEGFR2 in HUVECs (Supplementary Fig. S6; ref. 39). Finally, we showed that peretinoin inhibited canonical Wnt/β-catenin signaling by showing the decreased nuclear accumulation of β-catenin (Fig. 7). These data confirm the previous hypothesis of transrepression of the β-catenin promoter by 9cRA *in vitro* (40).

Although we showed that the PDGF signaling pathway is a target of peretinoin for preventing the development of hepatic fibrosis and tumors in mice, retinoid-inducing genes such as G0S2 (41), TGM2 (35), CEBPA (42), ATF, TP53BP, metallothionein 1H (MT1H), MT2A, and hemopexin (HPX) were upregulated in peretinoin-treated mice (data not shown). These canonical retinoid pathways are likely to participate in preventing disease progression in conjunction with anti-PDGF effects.

The precise mechanism of peretinoin toxicity, in which 5% of mice treated with 0.06% peretinoin died after 24 weeks of treatment, is currently under investigation. These mice showed severe osteopenia and we speculate that the toxicity might be caused by retinoid-induced osteopenia, as observed in a hypervitaminosis A rat model (43). However, the toxicity of prolonged treatment with oral retinoids in humans remains controversial (44) and severe osteopenia has so far only been seen in a rodent model.

In summary, we show that peretinoin effectively inhibits hepatic fibrosis and HCC development in *Pdgf-c Tg* mice. Further studies are needed to elucidate the detailed molecular mechanisms of peretinoin action and the effect of peretinoin on PDGF-C in human HCC. The recently developed multikinase inhibitor Sorafenib (BAY 43-9006, Nexavar) was shown to improve the prognosis of patients with advanced HCC (45). Promisingly, a phase II/III trial of peretinoin showed it to be safe and well tolerated (46). Therefore, combinatorial therapy that incorporates the use of small molecule inhibitors with peretinoin may be beneficial to some patients. The application of peretinoin during pre- or early-fibrosis stage could be beneficial in preventing the progression of fibrosis and subsequent development of HCC in patients with chronic liver disease.

Disclosure of Potential Conflicts of Interest

No potential conflicts of interest were disclosed.

Authors' Contributions

Conception and design: M. Honda, J.S. Campbell, S. Kaneko
Acquisition of data (provided animals, acquired and managed patients, provided facilities, etc.): H. Okada, M. Honda, J.S. Campbell, Y. Sakai, T. Yamashita, Y. Takebuchi, K. Hada, T. Shirasaki, R. Takabatake, M. Nakamura, H. Sunagozaka, N. Fausto
Analysis and interpretation of data (e.g., statistical analysis, biostatistics, computational analysis): J.S. Campbell, T. Yamashita, H. Sunagozaka, S Kaneko
Writing, review, and/or revision of the manuscript: H. OkadaM. Honda, J.S. Campbell, N. Fausto, S. Kaneko
Study supervision: J.S. Campbell, S. Kaneko
Pathologic examination and evaluation: T. Tanaka

Acknowledgments

The authors thank Dr. Scott Friedman, Mount Sinai School of Medicine (New York, NY), for providing Lx-2 cell lines and Nami Nishiyama and Masayo Baba for their excellent technical assistance.

Grant Support

This work was funded by NIH grants CA-23226, CA-174131, and CA-127228 (J.S. Campbell and N. Fausto). This work was also supported in part by a grant-in-aid from the Ministry of Health, Labour and Welfare, and KOWA Co., Ltd., Tokyo, Japan (M. Honda and colleagues).

The costs of publication of this article were defrayed in part by the payment of page charges. This article must therefore be hereby marked *advertisement* in accordance with 18 U.S.C. Section 1734 solely to indicate this fact.

Received January 9, 2012; revised April 27, 2012; accepted May 18, 2012; published OnlineFirst May 31, 2012.

References

1. Befeler AS, Di Bisceglie AM. Hepatocellular carcinoma: diagnosis and treatment. Gastroenterology 2002;122:1609–19.

2. Mohamed AE, Kew MC, Groeneveld HT. Alcohol consumption as a risk factor for hepatocellular carcinoma in urban southern African blacks. Int J Cancer 1992;51:537–41.

3. Tsukuma H, Hiyama T, Tanaka S, Nakao M, Yabuuchi T, Kitamura T, et al. Risk factors for hepatocellular carcinoma among patients with chronic liver disease. N Engl J Med 1993; 328:1797–801.
4. Deugnier YM, Charalambous P, Le Quilleuc D, Turlin B, Searle J, Brissot P, et al. Preneoplastic signi□cance of hepatic iron-free foci in genetic hemochromatosis: a study of 185 patients. Hepatology 1993;18:1363–9.
5. Yeoman AD, Al-Chalabi T, Karani JB, Quaglia A, Devlin J, Mieli-Vergani G, et al. Evaluation of risk factors in the development of hepatocellular carcinoma in autoimmune hepatitis: implications for follow-up and screening. Hepatology 2008;48:863–70.
6. Smedile A, Bugianesi E. Steatosis and hepatocellular carcinoma risk. Eur Rev Med Pharmacol Sci 2005;9:291–3.
7. Campbell JS, Hughes SD, Gilbertson DG, Palmer TE, Holdren MS, Haran AC, et al. Platelet-derived growth factor C induces liver □brosis, steatosis, and hepatocellular carcinoma. Proc Natl Acad Sci U S A 2005;102:3389–94.
8. Crawford Y, Kasman I, Yu L, Zhong C, Wu X, Modrusan Z, et al. PDGF-C mediates the angiogenic and tumorigenic properties of □broblasts associated with tumors refractory to anti-VEGF treatment. Cancer Cell 2009;15:21–34.
9. Lau DT, Luxon BA, Xiao SY, Beard MR, Lemon SM. Intrahepatic gene expression pro□les and alpha-smooth muscle actin patterns in hepatitis C virus induced □brosis. Hepatology 2005;42: 273–81.
10. Honda M, Yamashita T, Ueda T, Takatori H, Nishino R, Kaneko S. Different signaling pathways in the livers of patients with chronic hepatitis B or chronic hepatitis C. Hepatology 2006;44: 1122–38.
11. Muto Y, Moriwaki H, Ninomiya M, Adachi S, Saito A, Takasaki KT, et al. Prevention of second primary tumors by an acyclic retinoid, polyprenoic acid, in patients with hepatocellular carcinoma. Hepatoma Prevention Study Group. N Engl J Med 1996;334:1561–7.
12. Muto Y, Moriwaki H, Saito A. Prevention of second primary tumors by an acyclic retinoid in patients with hepatocellular carcinoma. N Engl J Med 1999;340:1046–7.
13. Suzui M, Masuda M, Lim JT, Albanese C, Pestell RG, Weinstein IB. Growth inhibition of human hepatoma cells by acyclic retinoid is associated with induction of p21(CIP1) and inhibition of expression of cyclin D1. Cancer Res 2002;62:3997–4006.
14. Sano T, Kagawa M, Okuno M, Ishibashi N, Hashimoto M, Yamamoto M, et al. Prevention of rat hepatocarcinogenesis by acyclic retinoid is accompanied by reduction in emergence of both TGF-alpha-expressing oval-like cells and activated hepatic stellate cells. Nutr Cancer 2005;51:197–206.
15. Muto Y, Moriwaki H, Omori M. In vitro binding af□nity of novel synthetic polyprenoids (polyprenoic acids) to cellular retinoid-binding proteins. Gann 1981;72:974–7.
16. Yamada Y, Shidoji Y, Fukutomi Y, Ishikawa T, Kaneko T, Nakagama H, et al. Positive and negative regulations of albumin gene expression by retinoids in human hepatoma cell lines. Mol Carcinog . 1994;10:151–8.
17. Honda M, Sakai A, Yamashita T, Nakamoto Y, Mizukoshi E, Sakai Y, et al. Hepatic ISG expression is associated with genetic variation in interleukin 28B and the outcome of IFN therapy for chronic hepatitis C. Gastroenterology 2010;139:499–509.
18. Frith C, Ward J, Turusov V. Pathology of tumors in laboratory animals. Vol. 2. Lyon, France: IARC Scienti□c Publications; 1994. p. 223–70.
19. Thoolen B, Maronpot RR, Harada T, Nyska A, Rousseaux C, Nolte T, et al. Proliferative and nonproliferative lesions of the rat and mouse hepatobiliary system. Toxicol Pathol 2010;38: 5S–81S.
20. Honda M, Takehana K, Sakai A, Tagata Y, Shirasaki T, Nishitani S, et al. Malnutrition impairs interferon signaling through mTOR and FoxO pathways in patients with chronic hepatitis C. Gastroenterology 2011;141:128–40, 140.e1–2.
21. Frith CH, Ward JM, Turusov VS. Tumours of the liver. IARC Sci Publ 1994;111:223–69.
22. Xu L, Hui AY, Albanis E, Arthur MJ, O'Byrne SM, Blaner WS, et al. Human hepatic stellate cell lines, LX-1 and LX-2: new tools for analysis of hepatic □brosis. Gut 2005;54:142–51.
23. Nhieu JT, Renard CA, Wei Y, Cherqui D, Zafrani ES, Buendia MA. Nuclear accumulation of mutated beta-catenin in hepatocellular carcinoma is associated with increased cell proliferation. Am J Pathol 1999;155:703–10.
24. Wong CM, Fan ST, Ng IO. beta-Catenin mutation and overexpression in hepatocellular carcinoma: clinicopathologic and prognostic significance. Cancer 2001;92:136–45.
25. van Zijl F, Mair M, Csiszar A, Schneller D, Zulehner G, Huber H, et al. Hepatic tumor-stroma crosstalk guides epithelial to mesenchymal transition at the tumor edge. Oncogene 2009;28: 4022–33.
26. Fischer AN, Fuchs E, Mikula M, Huber H, Beug H, Mikulits W. PDGF essentially links TGF-beta signaling to nuclear beta-catenin accumulation in hepatocellular carcinoma progression. Oncogene 2007;26: 3395–405.
27. Hou X, Kumar A, Lee C, Wang B, Arjunan P, Dong L, et al. PDGF-CC blockade inhibits pathological angiogenesis by acting on multiple cellular and molecular targets. Proc Natl Acad Sci U S A 2010;107: 12216–21.
28. Apte U, Zeng G, Muller P, Tan X, Micsenyi A, Cieply B, et al. Activation of Wnt/beta-catenin pathway during hepatocyte growth factor-induced hepatomegaly in mice. Hepatology 2006;44:992–1002.
29. Eguchi S, Kanematsu T, Arii S, Omata M, Kudo M, Sakamoto M, et al. Recurrence-free survival more than 10 years after liver resection for hepatocellular carcinoma. Br J Surg 2011;98:552–7.
30. Okusaka T, Ueno H, Ikeda M, Morizane C. Phase I and pharmacokinetic clinical trial of oral administration of the acyclic retinoid NIK-333. Hepatol Res 2011;41:542–52.
31. Okusaka T, Makuuchi M, Matsui O, Kumada H, Tanaka K, Kaneko S, et al. Clinical bene□t of peretinoin for the suppression of hepatocellular carcinoma (HCC) recurrence in patients with Child-Pugh grade A (CP-A) and small tumor: a subgroup analysis in a phase II/III randomized, placebo-controlled trial. J Clin Oncol 2011;29 Suppl 4s:165.
32. Araki H, Shidoji Y, Yamada Y, Moriwaki H, Muto Y. Retinoid agonist activities of synthetic geranyl geranoic acid derivatives. Biochem Biophys Res Commun 1995;209:66–72.
33. Nakamura N, Shidoji Y, Yamada Y, Hatakeyama H, Moriwaki H, Muto Y. Induction of apoptosis by acyclic retinoid in the human hepatoma-derived cell line, HuH-7. Biochem Biophys Res Commun 1995;207: 382–8.
34. Yasuda I, Shiratori Y, Adachi S, Obora A, Takemura M, Okuno M, et al. Acyclic retinoid induces partial differentiation, down-regulates telomerase reverse transcriptase mRNA expression and telomerase activity, and induces apoptosis in human hepatoma-derived cell lines. J Hepatol 2002;36:660–71.
35. Tatsukawa H, Sano T, Fukaya Y, Ishibashi N, Watanabe M, Okuno M, et al. Dual induction of caspase 3- and transglutaminase-dependent apoptosis by acyclic retinoid in hepatocellular carcinoma cells. Mol Cancer 2011;10:4.
36. Timke C, Zieher H, Roth A, Hauser K, Lipson KE, Weber KJ, et al. Combination of vascular endothelial growth factor receptor/platelet-derived growth factor receptor inhibition markedly improves radiation tumor therapy. Clin Cancer Res 2008;14: 2210–9.
37. Molander C, Hackzell A, Ohta M, Izumi H, Funa K. Sp1 is a key regulator of the PDGF beta-receptor transcription. Mol Biol Rep 2001;28: 223–33.
38. Bonello MR, Khachigian LM. Fibroblast growth factor-2 represses platelet-derived growth factor receptor-alpha (PDGFR-alpha) transcription via ERK1/2-dependent Sp1 phosphorylation and an atypical cis-acting element in the proximal PDGFR-alpha promoter. J Biol Chem 2004;279:2377–82.
39. Komi Y, Sogabe Y, Ishibashi N, Sato Y, Moriwaki H, Shimokado K, et al. Acyclic retinoid inhibits angiogenesis by suppressing the MAPK pathway. Lab Invest 2010;90:52–60.

40. Shah S, Hecht A, Pestell R, Byers SW. Trans-repression of beta-catenin activity by nuclear receptors. J Biol Chem 2003;278: 48137□45.
41. Kitareewan S, Blumen S, Sekula D, Bissonnette RP, Lamph WW, Cui Q, et al. G0S2 is an all-trans-retinoic acid target gene. Int J Oncol 2008;33:397□404.
42. Uray IP, Shen Q, Seo HS, Kim H, Lamph WW, Bissonnette RP, et al. Rexinoid-induced expression of IGFBP-6 requires RARbeta-dependent permissive cooperation of retinoid receptors and AP-1. J Biol Chem 2009;284:345□53.
43. Hough S, Avioli LV, Muir H, Gelderblom D, Jenkins G, Kurasi H, et al. Effects of hypervitaminosis A on the bone and mineral metabolism of the rat. Endocrinology 1988;122: 2933□9.
44. Ribaya-Mercado JD, Blumberg JB. Vitamin A: is it a risk factor for osteoporosis and bone fracture? Nutr Rev 2007;65: 425□38.
45. Llovet JM, Ricci S, Mazzaferro V, Hilgard P, Gane E, Blanc JF, et al. Sorafenib in advanced hepatocellular carcinoma. N Engl J Med 2008;359:378□90.
46. Okita K, Matsui O, Kumada H, Tanaka K, Kaneko S, Moriwaki H, et al. Effect of peretinoin on recurrence of hepatocellular carcinoma (HCC): results of a phase II/III randomized placebo-controlled trial. J Clin Oncol 2010;28 Suppl 15s:4024.

BMC Cancer

RESEARCH ARTICLE Open Access

Use of a chemically induced-colon carcinogenesis-prone *Apc*-mutant rat in a chemotherapeutic bioassay

Kazuto Yoshimi[1], Takao Hashimoto[2], Yusuke Niwa[2], Kazuya Hata[2], Tadao Serikawa[1], Takuji Tanaka[3] and Takashi Kuramoto[1*]

Abstract

Background: Chemotherapeutic bioassay for colorectal cancer (CRC) with a rat model bearing chemically-induced CRCs plays an important role in the development of new anti-tumor drugs and regimens. Although several protocols to induce CRCs have been developed, the incidence and number of CRCs are not much enough for the efficient bioassay. Recently, we established the very efficient system to induce CRCs with a chemically induced-colon carcinogenesis-prone *Apc*-mutant rat, Kyoto Apc Delta (KAD) rat. Here, we applied the KAD rat to the chemotherapeutic bioassay for CRC and showed the utility of the KAD rat.

Methods: The KAD rat has been developed by the ENU mutagenesis and carries a homozygous nonsense mutation in the *Apc* gene (S2523X). Male KAD rats were given a single subcutaneous injection of AOM (20 mg/kg body weight) at 5 weeks of age. Starting at 1 week after the AOM injection, they were given 2% DSS in drinking water for 7 days. Tumor-bearing KAD rats were divided into experimental and control groups on the basis of the number of tumors observed by endoscopy at week 8. The 5-fluorouracil (5-FU) was administrated intravenously a dose of 50 or 75 mg/kg weekly at week 9, 10, and 11. After one-week interval, the 5-FU was given again at week 13, 14, and 15. At week 16, animals were sacrificed and tumor number and volume were measured macroscopically and microscopically.

Results: In total 48 tumors were observed in 27 KAD rats with a 100% incidence at week 8. The maximum tolerated dose for the KAD rat was 50 mg/kg of 5-FU. Macroscopically, the number or volume of tumors in the 5-FU treated rats was not significantly different from the control. Microscopically, the number of adenocarcinoma in the 5-FU treated rats was not significantly different ($p < 0.02$) from that of the control. However, the volume of adenocarcinomas was significantly lower than in the control. Anticancer effect of the 5-FU could be obtained only after the 16 weeks of experimental period.

Conclusion: The use of the AOM/DSS-treated tumor-bearing KAD rats could shorten the experimental period and reduce the number of animals examined in the chemotherapeutic bioassay. The efficient bioassay with the AOM/DSS-treated tumor-bearing KAD rats would promote the development of new anti-tumor drugs and regimens.

Keywords: Adenomatous polyposis coli, Colorectal cancer, Endoscopy, Rat, Chemotherapy, 5-fluorouracil

* Correspondence: tkuramot@anim.med.kyoto-u.ac.jp
[1]Institute of Laboratory Animals, Graduate School of Medicine, Kyoto University, Yoshidakonoe-cho, Sakyo-ku, Kyoto 606-8501, Japan
Full list of author information is available at the end of the article

Background

Chemotherapeutic bioassays for colorectal cancer (CRC) play an important role in the development of new anti-tumor drugs and regimens. These bioassays involve the use of colon carcinogenesis models which mainly consist of animal xenografts, an adenomatous polyposis coli (*Apc*)-mutant mouse model and a chemically-induced CRC model [1-3].

The xenograft model utilizes cultured or primary CRC cells that are implanted under the skin of immune-deficient mice and rats. The size and volume of tumors can be estimated easily and temporally by measuring their dimensions. However, these animals have defects in the immune system that suppresses tumor growth. The subcutaneous microenvironment around the transplanted tumors differs from the colon environment in which the original CRC of the cell lines arose. Therefore, this approach appears to ignore the contribution of the tumor microenvironment and does not exactly mimic tumor development in man [4,5].

Apc-mutant mouse models, such as the Min mouse model, spontaneously develop a considerable number of intestinal tumors and have been widely used as a relevant model for evaluating human chemopreventative therapies. However, tumors in the colon are developed at a much lower frequency than in the small intestine. Even if tumors do develop in the colon, almost all of them are low grade adenomas [6].

The chemically-induced CRC model is superior to these models in that the characteristics of the induced tumor are very similar to those of human CRC. Tumors only develop in the colon through multi-step carcinogenesis which mimics the entire process of tumor growth in man. In this model, tumor morphology and mutation spectrum are also similar to those in human CRC [6]. Moreover, methods of inducing colon tumors are well-established, so that we can be certain of obtaining the number of tumors expected, which is ideal for the evaluation of potential chemotherapeutic drugs [2,7].

Although many carcinogens induce colon tumors in rats, azoxymethane (AOM) administered subcutaneously has been most widely used [2,6,8]. However, the incidence of colon tumors induced by two or three subcutaneous injections of AOM is not high, and it takes 7–9 months to induce sufficient tumors to evaluate the chemotherapeutic efficacy of potential anti-cancer drugs [9]. Such limitations have been significantly improved by using dextran sodium sulfate (DSS) as an inflammatory agent. When 2% DSS is administered in drinking water to the AOM-treated rats for one week, starting one week after administration, a number of colon tumors develop within a short time period (this is known as the TANAKA method) [10].

Recently we developed a novel *Apc* mutant rat strain, called the Kyoto Apc Delta (KAD) rat (strain name: F344-*Apc*^{m1kyo}) from our ENU-mutagenesis program. The KAD rat carries a homozygous nonsense mutation in the *Apc* gene (S2523X). Thus, the KAD rat lacks 321-amino acids in the C-terminal of APC, but it remains viable at almost 2 years and shows no spontaneous colorectal tumors. Moreover, by applying the TANAKA method to KAD rats, we obtained a much higher incidence, multiplicity and malignancy of colon tumors in KAD rats than colon tumors in F344 wild rats. We were able to induce these tumors within 15 weeks of the experimental period. In addition, we were able to carry out endoscopic observation, by which colon tumors could be detected from Week 8 [11].

In the present study, in order to establish an efficient chemotherapeutic bioassay with KAD rats, we induced colon tumors by means of treatment with AOM and DSS, and then administered a typical anti-tumor drug, namely 5-fluorouracil (5-FU) to the tumor-bearing rats.

Methods

Chemicals

5-FU was purchased from Kyowa Hakko Kogyo, Co., Ltd. (Tokyo, Japan). AOM was purchased from Sigma-Aldrich Chemical Co. (St. Louis, MO, USA). These drugs were diluted in saline just before administration. DSS (MW 36,000–50,000) was purchased from ICN Biochemicals, Inc. (Aurora, OH, USA). DSS was dissolved in distilled water at 2% (w/v) every day before treatment.

Rats

Specific pathogen free male KAD rats were purchased from Japan SLC, Inc. (Hamamatsu, Japan) and provided by the National Bio Resource Project for the Rat (http://www.anim.med.kyoto-u.ac.jp/nbr) at 4 weeks of age. The rats were acclimatized for a week before the experiment and were maintained under conditions of 50 ± 10% humidity, 12 h-12 h light cycle and 24 ± 2 °C temperature. They were fed a standard pellet diet (F-2, Funabashi Farm, Funabashi, Japan) and tap water *ad libitum*.

Induction of colon tumor

Chemically induced-colon carcinogenesis was carried out as described in our previous study [11]. Briefly, male KAD rats (n = 32) were given a single subcutaneous injection of AOM (20 mg/kg body weight) at 5 weeks of age. Starting at 1 week after the AOM injection, they were given 2% DSS in drinking water for 7 days (Figure 1). Five rats were used to find correlation of the number of polypoid lesions with the volume of tumors at Week 8. All experimental procedures were approved by the Animal Research Committee of Kyoto University

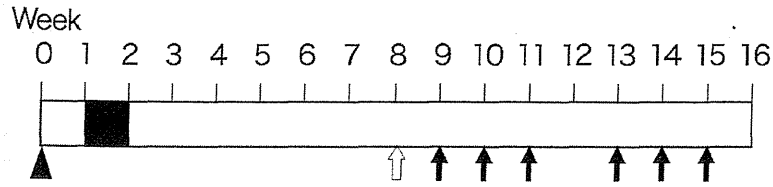

Figure 1 Experimental schedule. KAD rats at 5 weeks of age were given a subcutaneous injection of AOM at 20 mg/kg body weight (arrow head). One week after the AOM injection they were given 2% DSS (MW 36,000□50,000) in their drinking water for one week (black box). Endoscopic observation was carried out at week 8 (open arrow). 5-FU was administrated intravenously at weeks 9, 10, 11, 13, 14 and 15 (arrows). All animals were sacrificed at week 16.

and were performed according to the Regulation on Animal Experimentation at Kyoto University.

Endoscopic observation

Observation was performed at week 8 with an endoscope (BF TYPE 3C40: Olympus, Tokyo, Japan) to determine the presence of colon tumors (Figure 1). KAD rats were anesthetized by administration of 2% isoflurane (Forane: Abbott Japan, Tokyo, Japan) vapor through a nose cone. The colon was flushed using an enema of tap water to remove feces. The endoscope was inserted into the colon, and endoscopic images were acquired within the distal colon and rectum. The numbers of polypoid lesions, assumed to be developing colorectal tumors, were counted.

Chemotherapeutic test

The AOM/DSS-treated rats were divided into three groups (nine rats each), among which numbers of colon tumors were not significantly different. The 5-FU was administrated to the tumor-bearing KAD rats at two different doses (50 or 75 mg/kg) by three weekly intravenous (i.v.) injections at weeks 9, 10 and 11. According to the preliminary experiment, we set a 1 week withdrawal period to decrease the occurrence of serious side effects caused by 5-FU. One week later, rats underwent additional administration of 5-FU involving three weekly i.v. injections at weeks 13, 14 and 15. At week 16 animals were sacrificed by cervical dislocation under anesthesia with isoflurane (Figure 1). Then the colorectum of the rats was resected, washed with PBS, opened longitudinally along the main axis and fixed in 10% neutral buffered formalin for at least 24 h. The number and volume of colon tumors were measured after fixation. The other organs such as small intestine, stomach, liver and kidney were observed macroscopically for any abnormalities.

Histopathological examination

After careful macroscopic inspection, tumors and whole colonic mucosa were embedded in paraffin and sectioned for histopathology after staining with hematoxylin and eosin. After tumors that developed in the colorectum were photographed, the largest and the smallest superficial diameters of adenocarcinoma that were diagnosed histopathologically were measured on the photographs. Tumor volume was calculated according to the formula $V = a \times b^2/2$, in which "a" is the largest superficial diameter and "b" is the smallest superficial diameter [12].

Immunohistochemistry

Cell proliferation and apoptosis were evaluated by determination of the percentages of PCNA- and cleaved caspase-3-positive nuclei in a total of 200 cancer cells for each sample ($n = 6$ from the control group and $n = 8$ from Group 1). Briefly, sections were incubated with anti-mouse PCNA antibody (clone PC10, 1:1000 dilution; DAKO) and cleaved caspase-3 (Asp175) antibody (1:1000 dilution; Cell Signaling Technology) overnight at 4 °C. Biotinyl antibody was used as secondary antibody and then the streptavidin-peroxidase complex (LASB™ + Kit, Universal, DAKO) was applied. The antigen-antibody complex was visualized by 3,3⊖diamonobenzidine tetrachloride (DAKO).

Statistical analysis

Data are expressed as the mean ± standard deviation (S.D.). Student's *t*-test was performed using the statistics package within Microsoft Excel for statistical analysis, and p values were considered significant when < 0.05.

Results

Correlation of the number of polypoid lesions with the total volume of tumors

To find the correlation of the number of polypoid lesions with the total volume of tumors, we induced colon tumors to KAD rats ($n = 5$) by the TANAKA method and counted tumor number under the endoscopy and the number and volume of tumors under the microscopy at week 8 (Additional file 1: Table S1). As a good correlation between them was found, it is very likely that the number of polypoid lesions found with the endoscopy at week 8 can be used to estimate the total volume of tumors (Additional file 2: Figure S1).

Effective tumor development in AOM/DSS-treated KAD rats

At week 8 when carrying out endoscopic observations for the occurrence of colon tumors in the colons of AOM/DSS-treated KAD rats, we could observe about 10 cm of the luminal surface, from the rectum to the distal colon. We found polypoid lesions around the rectum and the distal colon. Polypoid lesions which were clearly different from normal mucosa assumed to be developing colorectal tumors. All AOM/DSS-treated KAD rats developed colon tumors. In total 48 tumors were observed in 27 KAD rats with a 100% incidence and a multiplicity of 1.78 ± 0.85, ranging from 1 to 4 per rat.

Dosing condition of 5-FU

On the basis of the number of tumors, the tumor-bearing KAD rats were divided into three groups. One was the control group and the others were experimental groups, in which rats were given 5-FU at a concentration of 50 mg/kg (Group 1) or 75 mg/kg (Group 2). Each group consisted of nine rats and the total number of tumors in each group was 16. The average number of tumors per rat was not significantly different among the groups (Control: 1.78 ± 0.83, Group 1: 1.78 ± 0.83, Group 2: 1.78 ± 0.97) (Figure 2B).

The average body weight of rats in Group 1 tended to be lower than in the control group, and was significantly different from the control group at weeks 15 (300.0 ± 18.1 vs 319.4 ± 20.1; $p < 0.05$) and 16 (296.1 ± 18.9 vs 318.8 ± 18.8; $p < 0.03$). However the reduction in body weight was less than 10% as compared with the control. None of the rats in Group 1 died during the experiment. On the other hand, gain in body weight in Group 2 was constantly and significantly impaired throughout the experimental period. More than 10% of weight loss was observed at weeks 12, 15 and 16, as compared with that in the control group (Figure 3A). KAD rats in Group 2 had severe bloody stools and diarrhea and six rats (67%) in the group died during the experiment (Figure 3B). These findings indicated that the 75 mg/kg dose of 5-FU was too toxic for the tumor-bearing KAD rats, and led to the marked body weight loss and eventually to death. Thus, the 50 mg/kg dose of 5-FU was considered to be appropriate for evaluation of the antitumor activity of 5-FU, when we used the tumor-bearing KAD rats in a chemotherapeutic bioassay.

Reduction of volume but not number of adenocarcinomas in the tumor-bearing KAD rats by treatment with 5-FU

At week 16 we carried out an autopsy and macroscopic examination of the large bowels of the control group and Group 1. Macroscopically, rats in both groups developed multiple nodular, polypoid or caterpillar-like tumors mainly in the rectum and distal colon (Figure 4). The number of tumors in Group 1 was not significantly different from the control group (Table 1). The volume of tumors, which were macroscopically calculated, was 27% smaller in Group 1 than in the control group, but the difference was not significant ($p = 0.34$).

Microscopically, all tumors that developed in KAD rats were tubular adenoma or well- or moderately-differentiated tubular adenocarcinoma (Figure 5A and 5B). The multiplicity of adenoma or adenocarcinoma in Group 1 was not significantly different from that of the control group ($p = 0.53$; $p = 0.44$, respectively) (Table 1). The size of the adenomas was too small for their volumes to be calculated. However, the volume of adenocarcinomas (63.85 ± 51.06 mm^3) in Group 1 was significantly lower ($p < 0.02$) than in the control group (34.40 ± 31.26 mm^3), when the volume was calculated from the histological sections. In addition, we found significant reduction of PCNA labeling index as well as

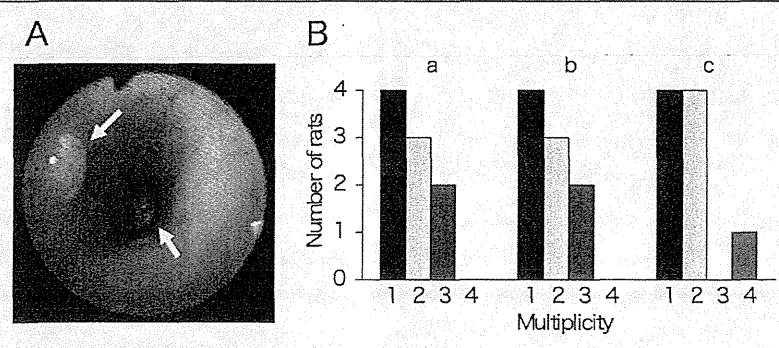

Figure 2 Grouping of AOM/DSS-treated KAD rats before 5-FU treatment. (**A**) Endoscopic view of colon tumors (arrows) in an AOM/DSS-treated KAD rat at week 8. (**B**) AOM/DSS-treated KAD rats were divided into experimental groups based on the number of tumors induced in their colons. The number of tumors induced in each animal determined by endoscopic observations varied from one to four. In total, 48 tumors were found in 27 rats. The tumor-bearing rats (nine per group) were divided into three groups (a: saline, b: 50 mg/kg 5-FU and c: 75 mg/kg 5-FU), so as not to be significantly different at the starting point of treatments.